Contents list available at CBIORE journal website

International Journal of Renewable Energy Development

Journal homepage: https://ijred.cbiore.id

Research Article

Development of hybrid COA-WCA multi-objective optimization of microgrid hybrid renewable energy system: A case study of Nusa Penida

Ida Bagus Ketut Sugirianta[a,b], Ida Ayu Dwi Giriantari[a*], Wayan Gede Ariastina[a], Ida Bagus Alit Swamardika[a]

[a]*Study Program of Doctoral Engineering Science (PSDIT), Udayana University, Bali, Indonesia*

[b]*Department of Electrical Engineering, Politeknik Negeri Bali (PNB), Bali, Indonesia*

Abstract. This study proposes a hybrid metaheuristic that combines the Coyote Optimization Algorithm (COA) and the Water Cycle Algorithm (WCA) to improve multi-objective optimization of a hybrid renewable energy microgrid (HRES) for Nusa Penida Island. Such islanded systems must balance investment cost, operational reliability, and renewable curtailment while facing stochastic weather and demand. The optimization therefore targets simultaneous minimization of cost of energy (COE), loss of power supply probability (LPSP), and dummy load (DL) as key indicators of affordability, adequacy, and energy-utilization efficiency. A sequential Hybrid COA–WCA framework is implemented using an annual time-series of electrical demand and local renewable-resource profiles. Candidate solutions encode the main HRES components, including photovoltaic generation, wind generation, battery storage, and conventional backup biodiesel generation, while respecting practical operating limits. Multi-objective optimization is handled using a weighted-sum formulation, subject to standard power-balance, component-operating, and reliability constraints. The proposed approach is benchmarked against standalone COA, WCA, and WOA under multiple uncertainty scenarios that perturb techno-economic parameters and resource–load conditions. The Hybrid COA–WCA achieved the lowest mean objective value (mean f = 0.87274; min = 0.82136; max = 0.92409) and the best final-iteration mean of 0.87258 compared with COA (0.87303), WCA (0.87367), and WOA (0.87756). The optimized design delivered COE = 1.388, LPSP = 0.03180, and DL = 6,609.025 on average across scenarios. Robustness analysis also indicates faster stabilization and the smallest end-of-run fluctuation range (0.82136–0.92409), confirming improved convergence stability relative to the benchmark algorithms. Overall, the Hybrid COA–WCA provides a stable and competitive optimization approach for HRES sizing under uncertainty, yielding consistently high-quality solutions that support planning and decision-making for island microgrids.

Keywords: cost of energy; dummy load; hybrid renewable energy systems; loss of power supply probability; multi-objective optimization; nusa penida

Received: 26th Dec 2025; Revised: 17th April 2026; Accepted: 7th May 2026; Available online: 14th May 2026

1. Introduction

The global transition toward a sustainable and low-carbon energy system has become a top priority in the 21st century. The drive for decarbonization and energy security has intensified efforts to utilize renewable energy sources (RES) such as solar photovoltaic (PV), wind turbines (WT), biomass, and hydrogen. However, the inherent intermittency and variability of these resources introduce significant technical and operational challenges, particularly in maintaining grid stability, ensuring supply reliability, and achieving cost efficiency (Azeem *et al.*, 2021; Lei *et al.*, 2023). To address these limitations, hybrid renewable energy microgrid systems (HRES) have emerged as a strategic architecture capable of integrating diverse power sources and energy storage systems to ensure continuous power delivery, whether operating in grid-connected or islanded modes

HRES plays a significant role in enabling higher penetration of renewable energy, enhancing resilience against power fluctuations, and reducing carbon emissions (Mirtaheri *et al.*, 2021; Wang *et al.*, 2024). The deployment of HRES is particularly relevant for remote-area electrification, smart city development, and industrial decarbonization. Consequently, the optimization of microgrids powered by 100% renewable energy has received substantial attention, as it represents a strategic pathway toward achieving a net-zero energy system aligned with the Sustainable Development Goals (SDGs) (Bhatti *et al.*, 2024).

International bibliometric reports and surveys conducted between 2020 and 2025 indicate an exponential increase in research on the technical and economic optimization of hybrid microgrids. This trend is supported by advancements in modeling tools such as HOMER Pro and the FORCE Toolkit, the development of multi-scale energy management systems, and improved capabilities for predicting renewable energy

* Corresponding author
Email: dayu_giriantari@unud.ac.id (I.A.D. Giriantari)

https://doi.org/10.61435/ijred.2026.62158
ISSN: 2252-4940/© 2026.The Author(s). Published by CBIORE

intermittency (Williams and Chang, 2024). Furthermore, co-design approaches that integrate economic and control perspectives have gained increasing attention as a means to ensure long-term reliability and system sustainability. Case studies in rural and coastal regions demonstrate that hybrid configurations combining PV, WT, battery storage, and biodiesel can achieve competitive Levelized Cost of Energy (LCOE) values (Akter *et al.*, 2021; Tjahjana *et al.*, 2023). Therefore, the integration of optimization techniques and advanced energy forecasting has become a key research direction in supporting the global transition toward microgrid systems powered entirely by renewable energy (Zhong *et al.*, 2020; Mquqwana and Krishnamurthy, 2024).

Despite substantial advancements, the optimization of microgrids powered entirely by renewable energy continues to face multidimensional challenges encompassing technical, economic, and operational aspects. The primary challenge lies in the system's ability to simultaneously manage intermittency, variability, and multi-objective trade-offs across different time scales, from long-term planning and daily scheduling to real-time control (Billah *et al.*, 2023). The inherently stochastic nature of renewable energy further necessitates multi-scale optimization models that accurately represent system behavior while avoiding excessive computational complexity (Jaiswal *et al.,* 2025).

Furthermore, frequency stability has become a critical issue due to the declining system inertia in microgrids dominated by inverter-based generation. The absence of traditional synchronous generators leads to significant frequency deviations during electrical disturbances. This condition necessitates the implementation of virtual inertia control strategies and coordinated hybrid energy storage systems (ESS), such as battery–supercapacitor or battery–hydrogen combinations, to ensure fast and efficient frequency recovery. The optimal design of ESS capacity is also essential, as it is directly related to battery degradation, life-cycle cost, and long-term system reliability (Sharma and Prabhakar, 2021; Lei *et al.*, 2023).

Operational uncertainty has added another layer of complexity to microgrid optimization. Microgrids, whether islanded or grid-connected, must adapt to fluctuating meteorological conditions, volatile market prices, and uncertainties in energy demand (Zaheri, Hosseini and Fathinasab, 2024). The increasing penetration of electric vehicles (EVs) and vehicle-to-grid (V2G) technologies further introduces uncertainties related to charging schedules, energy availability, and bidirectional power flows (Boukaibat *et al.*, 2025). Deterministic models such as Mixed-Integer Linear Programming (MILP) remain widely used due to their numerical robustness however, they have inherent limitations in capturing the nonlinear characteristics of microgrid systems (Tarife et al., 2022). While stochastic approaches provide more realistic representations of uncertainty, they often require a large number of scenarios, which can lead to a "computational explosion" (Dabhi and Pandya, 2020). Consequently, current research trends are shifting toward hybrid and intelligent approaches that integrate data-driven learning, predictive modeling, and optimization within an adaptive computational framework.

Metaheuristic algorithms have emerged as a highly promising approach for solving complex optimization problems in hybrid microgrid systems. These algorithms, which are inspired by natural biological and physical phenomena such as Particle Swarm Optimization (PSO), Genetic Algorithm (GA), Grey Wolf Optimization (GWO), and Water Cycle Algorithm (WCA), have been widely applied for component sizing, operational scheduling, and energy management (Kharrich *et al.*, 2020; Ullah *et al.*, 2023). However, each algorithm has inherent limitations, including premature convergence to local optima, high sensitivity to initial parameters, and the absence of guarantees for global optimality (Bose and Auxillia, 2021; Hossam-Eldin *et al.*, 2022). To address these challenges, hybrid metaheuristic algorithms have gained significant attention because they combine two or more complementary methods to achieve a more effective balance between global exploration and local exploitation (Cetinbas *et al*, 2022; Charadi *et al.*, 2023).

Recent literature shows that hybrid algorithms consistently achieve better performance than single algorithms when solving large-scale multi-objective optimization problems. For example, Suman (2021) combined PSO and GWO to optimize the sizing and operation of a photovoltaic-wind-biogas-diesel hybrid system, resulting in significant improvements in convergence speed and solution diversity. A similar approach was implemented by Dey et al. (2020) and Balasubramanyam and Sood (2023), who integrated bio-inspired and swarm intelligence algorithms to enhance system stability and efficiency.

However, the combination of the Coyote Optimization Algorithm (COA) and the Water Cycle Algorithm (WCA) has been explored only in limited studies. COA, which mimics the social behavior and adaptive pack dynamics of coyotes, performs well in fast local exploitation and adapts effectively to environmental dynamics (Upadhyay and Bhasker, 2025). On the other hand, WCA, which imitates the natural water cycle process, has a strong capability for global exploration and offers fast convergence (Eskandar *et al.*, 2012). The combination of COA and WCA offers a more effective balance between exploration and exploitation by addressing the limitations of each individual algorithm in solving complex microgrid optimization problems (Charadi, et al., 2023).

The hybrid COA-WCA approach shows considerable potential for solving multi-objective optimization problems in 100% renewable energy microgrid systems, where a trade-off must be achieved among three principal objectives: minimizing the cost of energy (COE), minimizing the Loss of Power Supply Probability (LPSP), and reducing dummy load (DL). The adaptive capability of COA, combined with the global exploration strength of WCA, offers improvements in convergence speed, result stability, and solution diversity under stochastic operating conditions. When integrated with scalarization techniques such as the Weighted Sum Method (WSM), the hybrid algorithm can generate Pareto-optimal solutions that balance economic, technical, and robustness considerations (Marler and Arora, 2010; Bazgan *et al.*, 2022; Helfrich *et al.*, 2022).

Even though metaheuristic hybridization has become increasingly popular, most previous studies remain empirical and lack a strong theoretical foundation. Therefore, the development of an analytically structured COA–WCA algorithm can help reduce this gap. Unlike classical hybrid combinations, such as PSO–GA or GA–SA, the integration of COA and WCA leverages the adaptive capabilities of COA together with the global exploration strength of WCA to efficiently solve large, complex, and constrained search spaces (Balasubramanyam and Sood, 2023; Charadi et al., 2023).

This study aims to develop and validate a multi-objective hybrid COA-WCA algorithm specifically designed to optimize component sizing and energy management in hybrid renewable energy microgrid systems. The proposed approach integrates the local exploitation capability of COA and the global

exploration capability of WCA within a balanced and sequential optimization framework. This study contributes at three main levels: (i) theoretical, through the formulation and convergence analysis of the hybrid COA-WCA operator; (ii) methodological, through the integration of a multi-objective hybrid optimization approach with mechanisms to handle uncertainty; and (iii) application, through demonstrating the superiority of the proposed algorithm in a real-world case study involving a PV-wind-BESS-biodiesel generator system. Thus, this research provides a reliable, efficient, and scalable optimization framework for the design and operation of sustainable hybrid microgrid systems, while supporting broader efforts toward a resilient and low-carbon energy future.

2. Optimization Algorithm in Hybrid Microgrid Renewable Energy System

2.1 Concept and evolution of renewable energy-based hybrid microgrid systems

A Hybrid Renewable Energy System (HRES) is an integrative approach that combines multiple renewable energy sources, such as solar power, wind energy, and biomass, together with energy storage systems (ESS) and backup units (backup generators), within a coordinated local network (Billah *et al.*, 2023; Naseri *et al.*, 2024). An HRES can operate either in islanded mode, functioning independently without connection to the main grid, or in grid-connected mode, where it interacts with the main network. HRES configurations have been shown to improve supply reliability, reduce carbon emissions, and decrease dependence on fossil fuels (Alsharif *et al.*, 2023).

The complexity of HRES architectures continues to increase with the advancement of energy storage technologies and the growing integration of electric vehicles (EVs) and vehicle-to-grid (V2G) systems. An HRES is no longer merely a power generator it also functions as a prosumer capable of supplying power back to the grid. This condition requires advanced control strategies and optimization methods to ensure efficient, stable, and economically viable operation (Singla *et al.*, 2023). Consequently, recent studies have increasingly focused on integrated optimization frameworks that encompass component sizing, operational scheduling, energy management, as well as control and protection systems (Arul *et al.*, 2024; Azeem *et al.*, 2025).

Conceptually, HRES plays a critical role in supporting the global energy transition toward 100% renewable energy, as it integrates operational flexibility, energy efficiency, storage component degradation management, and real-time load–supply balancing across multiple time scales (Lei *et al.*, 2023; Hussein *et al.*, 2024).

2.2 Key Areas of Optimization in Hybrid Microgrid Systems

Renewable energy–based microgrid optimization studies can generally be classified into three main domains: (1) design optimization and component sizing, (2) optimization of the energy management system (EMS), and (3) optimization of control parameters and protection systems (Aljohani, Ebrahim and Mohammed, 2020; Hossain *et al.*, 2022; Bakeer *et al.*, 2023). Sizing optimization aims to determine the optimal capacity of each system component, such as PV, WT, battery storage, and backup generators, in order to achieve the lowest Net Present Cost (NPC) and cost of energy (COE) without compromising system reliability (Twala *et al.*, 2023). Meanwhile, EMS optimization focuses on multi-period scheduling strategies to minimize operational costs and enhance the utilization of renewable energy sources (Fracas *et al.*, 2022).

Control and protection optimization is an essential aspect for maintaining frequency, voltage, and power quality stability, particularly during islanded operation or during grid-connection and disconnection transitions (Alahakoon, Roy and Arachchillage, 2023; Tripathi *et al.*, 2023). Research in this domain includes the development of droop control, model predictive control (MPC), and virtual inertia control to address low-inertia challenges resulting from the dominance of inverter-based generators (Senarathna and Hemapala, 2020; Ebrahim *et al.*, 2024).

2.3 Metaheuristic Algorithms in Microgrid Optimization

Optimization problems in hybrid microgrid systems are inherently nonlinear, nonconvex, multi-objective, and often involve discrete variables. These characteristics make conventional deterministic methods, such as Mixed-Integer Linear Programming (MILP) or Linear Programming (LP), difficult to apply effectively. Consequently, metaheuristic algorithms have become a popular alternative due to their ability to efficiently navigate large solution spaces without requiring derivative information or convexity assumptions (Kharrich *et al.*, 2020; Ullah *et al.*, 2022).

Several metaheuristic algorithms have been widely applied in microgrid optimization, including Particle Swarm Optimization (PSO), Genetic Algorithm (GA), Grey Wolf Optimization (GWO), Artificial Bee Colony (ABC), Moth-Flame Optimization (MFO), and the Water Cycle Algorithm (WCA) (Hossain et al., 2022; Tarife et al., 2022). Metaheuristic methods offer near-optimal solutions within relatively short computational times. However, they also have inherent limitations, such as premature convergence, sensitivity to initial parameter settings, and non-deterministic outcomes (Bose and Auxillia, 2021; Akinwola and Alkuhayli, 2025). As the complexity of HRES continues to increase, there is a growing need for optimization methods capable of simultaneously handling multi-objective formulations and stochastic uncertainties, while also offering high scalability for real-time operation (Ibrahim *et al.*, 2023; Spiegel and Strasser, 2023).

2.4 Trends in Hybridization of Metaheuristic Algorithms

Recent developments indicate a paradigm shift from single metaheuristic algorithms toward hybrid approaches, which combine two or more methods to simultaneously leverage global exploration and local exploitation capabilities (Cetinbas et al., 2022 ; Charadi et al., 2023). For example, hybrid ICA–PSO has been shown to improve convergence speed and result stability in economic microgrid optimization (Charadi et al., 2023), while combinations such as HHO-AOA and Swarm-Cuckoo Search (CS) have demonstrated significant improvements in solution quality and adaptability under uncertainty (Balasubramanyam and Sood, 2023; Dey and Xu, 2023). These hybrid approaches integrate the global exploration capability of the first algorithm (for instance, PSO or WCA) with the strong local exploitation capability of the second algorithm (such as GA or COA).

The advantages of hybridization lie in its ability to prevent stagnation in local optima, accelerate convergence, and maintain solution diversity. In the context of microgrids, hybrid algorithms have been shown to be highly effective in solving multi-objective optimization problems involving conflicting

criteria such as cost, emissions, and reliability (Zhong *et al.*, 2020; Hossain *et al.*, 2022).

2.5 Potential and Advantages of the Hybrid COA–WCA Algorithm

Recent literature indicates that metaheuristic hybridization not only improves convergence speed and stability but also enhances the ability of algorithms to address multi-objective optimization and stochastic operating conditions (Charadi et al., 2023). The COA–WCA hybrid provides an effective balance between search speed and exploitation depth while maintaining population diversity to reduce the risk of premature convergence to local optima.

In addition, the application of the hybrid COA–WCA algorithm in 100% renewable energy–based hybrid microgrid systems enables seamless integration with scalarization techniques such as the Weighted Sum Method (WSM). This method is used to transform multiple conflicting objectives, such as cost of energy (COE), Loss of Power Supply Probability (LPSP), and dummy load (DL), into a single aggregated objective function that can be optimized simultaneously (Marler and Arora, 2010; Bazgan *et al.*, 2022) .

Through this approach, the system optimization process can generate a Pareto front that presents a range of efficient solution alternatives, enabling decision-makers to select the most suitable configuration based on economic, reliability, or environmental priorities.

Compared with other hybrid algorithms, such as ICA–PSO, HHO–AOA, or hybrid Swarm–CS, the COA–WCA approach offers unique advantages. The adaptive social structure of COA allows the search direction to be adjusted dynamically based on environmental feedback, while the evaporation and infiltration mechanisms in WCA help prevent search stagnation and broaden the exploration of the solution space. These characteristics make COA–WCA potentially superior for solving large-scale optimization problems under strict computational constraints (Charadi, et al., 2023; Upadhyay and Bhasker, 2025).

2.6 Research Gap and Development Direction

Although various hybrid algorithms have been evaluated in the context of microgrid optimization, such as ICA–PSO and HHO–AOA, studies examining the combination of COA and WCA remain very limited in the existing literature (Cetinbas et al. 2022; Charadi et al., 2023).Most previous research has focused on the application of COA for specific tasks, such as Maximum Power Point Tracking (MPPT) or controller tuning, rather than for comprehensive multi-objective optimization in hybrid microgrid systems (Upadhyay and Bhasker, 2025).

Accordingly, there is a clear research gap regarding the use of COA-WCA for integrated optimization that encompasses design aspects (sizing), Energy Management Systems (EMS), and real-time control. In addition, only a few studies have analytically examined the convergence stability and computational complexity of the hybrid COA-WCA approach, even though such analyses are essential to ensure the practical implementability of the algorithm in real-world energy systems. Therefore, this study aims to develop a hybrid COA-WCA model that is theoretically structured, methodologically integrated, and validated through a real case study. This approach strengthens the scientific foundation of hybrid metaheuristic algorithms and contributes to improving the efficiency, reliability, and sustainability of renewable energy systems.

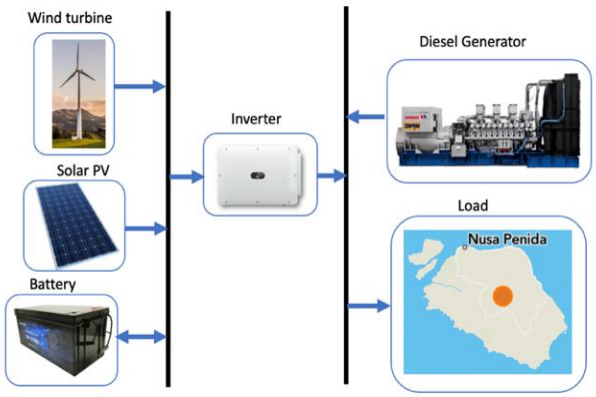

Fig. 1 Schematic configuration of the proposed hybrid microgrid system

3. Materials and methods

This section describes the materials and methods used in this study to develop and evaluate the Hybrid COA–WCA optimization algorithm for a renewable energy–based hybrid microgrid system. The materials include the configuration and components of the hybrid microgrid, as well as the data from Nusa Penida Island in Bali, which serves as the case study. The methods implemented in this study follow a systematic approach consisting of four main steps: (1) system modeling, (2) formulation of the multi-objective optimization functions, (3) design and implementation of the sequential hybrid COA-WCA algorithm, and (4) performance simulation and evaluation. This methodological framework integrates HRES component sizing to address the technical and economic challenges associated with the energy system of Nusa Penida Island.

3.1 Hybrid Microgrid System Components

This study designs a hybrid microgrid system that integrates several key components, including photovoltaic (PV) solar modules, wind turbines, battery energy storage, and a diesel generator. The system is designed to utilize the strong solar potential and abundant wind resources available in Nusa Penida. By combining renewable energy sources with a reserve diesel generator, the proposed system aims to provide a sustainable and reliable electricity supply for Nusa Penida Island, reduce dependence on fossil fuels, and optimize the utilization of local renewable resources. Despite the intermittent nature of solar and wind energy, the combination of these sources with energy storage ensures stable power generation. The biodiesel generator functions as a reserve unit to maintain network stability when renewable production is insufficient. Fig. 1 illustrates the schematic configuration of the proposed hybrid microgrid system.

3.2 Nusa Penida Island

Located in the Klungkung Regency of Bali, Nusa Penida Island is selected as the case study for this study. The island lies to the south of Bali and covers an area of approximately 209.4 km², with a total population of 62,082 as of 2021. The geographical location of Nusa Penida Island, situated about 20 km southeast of Denpasar, Bali, Indonesia. In 2023, the electrical peak load of Nusa Penida reached approximately 11.3 MW. The current electricity supply is generated by seven diesel-powered power plants with a total capacity of 10 MW, eleven genset units with

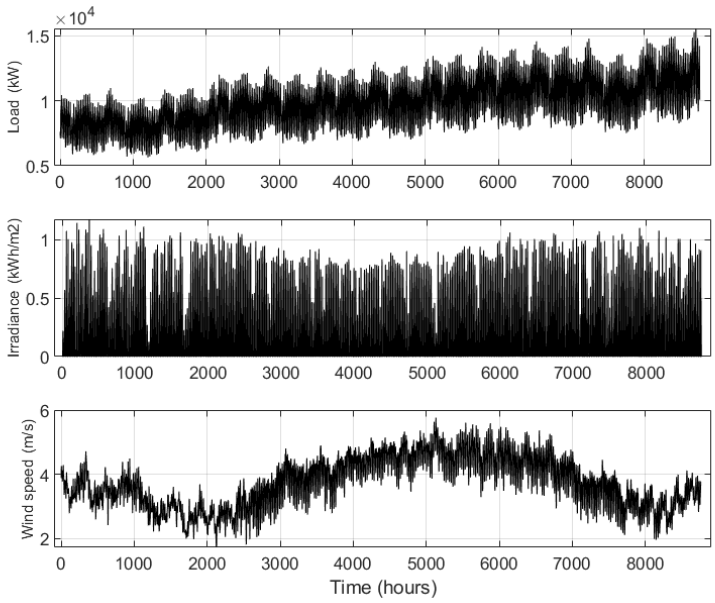

Fig. 2 Annual profiles of electrical load, solar irradiation, and wind speed on Nusa Penida Island

a combined capacity of 1,657 kVA, a 3.5 MW ground-mounted solar power plant, and a 1 MW battery energy storage system (BESS) (CORE Udayana, 2024). Nusa Penida is widely recognized for its natural beauty and biodiversity, and it has become one of Bali's most popular tourist destinations. Despite this, the island continues to face significant challenges in achieving sustainable energy development. To address these issues, several renewable energy initiatives and projects are being considered for implementation on Nusa Penida Island.

The annual electrical load profile of Nusa Penida shows a consistently increasing trend, with a minimum value of 5,865 kWh (at t = 37) and a maximum value of 16,323 kWh (at t = 8,430). The average daily load is approximately 11,215 kWh. This fluctuation reflects rising energy demand, which is closely associated with population growth, tourism activity, and seasonal variations. The increase in peak loads toward the end of the year also suggests a potential correlation with seasonal tourism surges, highlighting the need for careful planning to enhance grid resilience and ensure the long-term sustainability of the island's energy supply. Fig. 2 displays annual data (8760 hours) of the characteristics of electrical load, solar irradiation and wind speed in Nusa Penida.

The solar energy potential of Nusa Penida Island is relatively well distributed throughout the year, with Global Horizontal Irradiance (GHI) values ranging from 4.8 to 5.6 kWh/m²/day and relatively low rainfall, particularly from May to October. According to the Institute for Essential Services Reform (IESR, 2021) in the report Beyond 443 GW – *Indonesia's Infinite Renewable Energy Potentials*, the maximum potential for utility-scale solar power plants on Nusa Penida is estimated to reach 3.2 GW, based on the total land area suitable for large-scale PV development. For rooftop solar PV, and assuming that each 1 kWp installation requires an average roof area of 5.76 m², the total rooftop PV potential on Nusa Penida is estimated to reach 10,965 MWp, based on the distribution of roof areas across different building types (CORE Udayana, 2024).

The wind speed profile on Nusa Penida Island exhibits notable temporal variation. The lowest wind speed occurs in March, at 1.72713 m/s (t = 2.125), while the highest value is recorded in August, reaching 5.7652 m/s (t = 5.133). This pattern indicates favorable wind conditions for turbine operation during the mid-year period. The average wind speed is 3.7247 m/s, which is higher than the typical cut-in speed of 2.5 m/s. Therefore, wind turbines provide relatively consistent electricity generation throughout the year.

3.3 Hybrid Microgrid System Modeling

The first step in the methodology is the design of a Hybrid Renewable Energy System (HRES) that includes photovoltaic (PV) modules, wind turbines (WT), batteries as energy storage systems (ESS), and biodiesel generators (BDG). The model accounts for the intermittent nature of renewable resources and aims to ensure a continuous energy supply through appropriate component sizing and energy management. The system is developed to simulate a microgrid that utilizes the abundant solar and wind resources available on Nusa Penida Island. The objective is to evaluate how the COA-WCA algorithm optimizes the sizing and operation of these components to minimize costs, improve reliability, and maximize the use of renewable energy. In a hybrid microgrid (HRES) system, it is essential to quantify the total energy generated by all components, including solar PV, wind turbines, batteries, and biodiesel generators. The potential energy output from each component can be evaluated using appropriate mathematical and computational models.

3.3.1 Solar PV

The electrical power generated by a solar module depends on the module characteristics, solar irradiance $\boldsymbol{G}$(W/m²), and cell temperature $\boldsymbol{T_c}$(°C), and can be calculated using Equation (1) (Janamala and Reddy, 2021).

$$P_{PV}(t) = \eta_{ref}\eta_{inv}\left[1 - \beta_c\left\{T_{a(t)} + G_{(t)}\left(\frac{NOCT-20}{800}\right) - T_{ref}\right\}\right]N_m A_m G_{(t)} \quad (1)$$

Where $\boldsymbol{P_{PV}(t)}$, $\boldsymbol{\eta_{ref}}$, $\boldsymbol{\eta_{inv}}$, $\boldsymbol{\beta_c}$, $\boldsymbol{T_{a(t)}}$, $\boldsymbol{T_{ref}}$, $\boldsymbol{N_m}$, $\boldsymbol{A_m}$, $\boldsymbol{G}$, $\boldsymbol{G_0}$, and NOCT denote, respectively, the estimated power generated by the PV system (W), the reference efficiency under Standard Test Conditions (STC) (%), the inverter efficiency (%), the

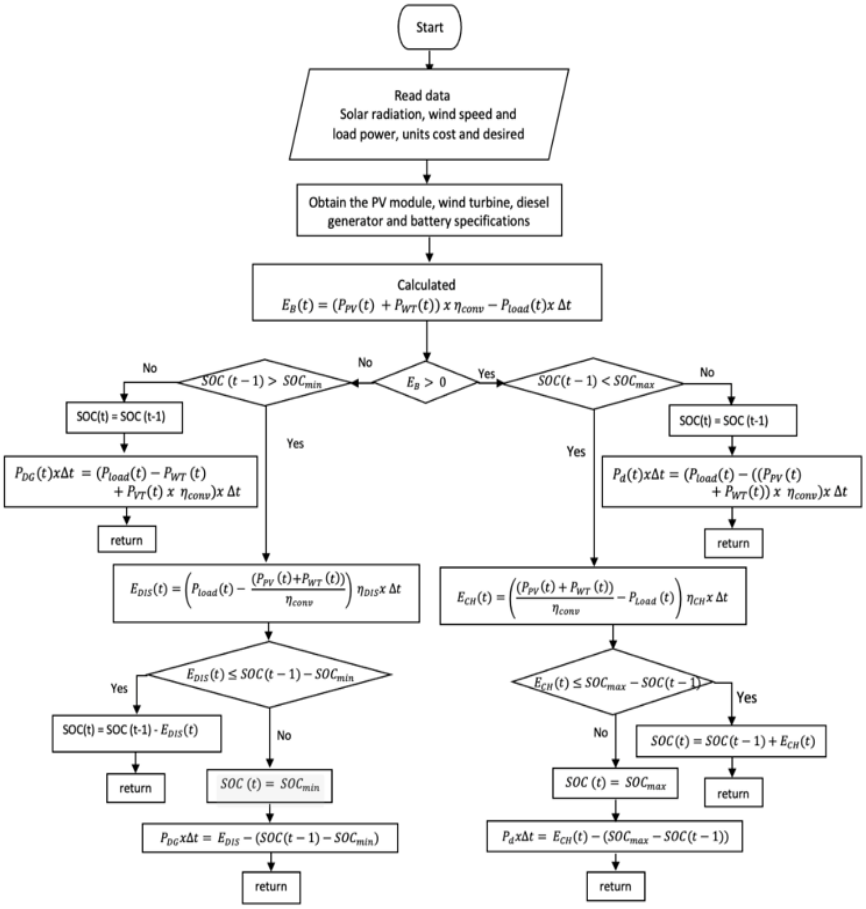

Fig. 3 Power flow flowchart of hybrid microgrid system

temperature coefficient (typically 0.004–0.006 per °C for silicon-based cells), the ambient temperature (°C), the module temperature under STC (°C), the number of PV modules in the system (units), the surface area of a solar module (m²), the solar irradiance incident on the module surface (W/m²), the irradiance under STC (W/m²), and the Nominal Operating Cell Temperature (NOCT), which represents the cell temperature when the PV module operates at 800 W/m² irradiance and 20°C ambient temperature, typically ranging from 42°C to 46°C.

3.3.2 Wind turbine

The power output of a wind turbine (WT) can be calculated and estimated using Equations (2)–(4) (Singh and Fernandez, 2018).

$$P_{wt} = 0 \quad jika \;\; V < Vcut_{in} \;\; or \;\; V > Vcut_{out} \tag{2}$$

$$P_{wt} = V^3 \left(\frac{P_r}{{V_r}^3 - {Vcut_{in}}^3}\right) - \left(\frac{{Vcut_{in}}^3}{{V_r}^3 - {Vcut_{in}}^3}\right) \Pr \tag{3}$$

$$if \;\; V > Vcut_{in} \;\; and \;\; V < V_r$$

$$P_{wt} = P_r \quad if \;\; V > V_r \;\; and \; V < Vcut_{out} \tag{4}$$

Where P_{WT}, P_r, V_r, V, $V_{cut\text{-}in}$, and $V_{cut\text{-}out}$ denote, respectively, the power generated by the wind turbine (kW), the rated power of the wind turbine (kW), the rated wind speed (m/s), the measured wind speed (m/s), the cut-in wind speed (m/s), and the cut-out wind speed (m/s).

3.3.3 Battery

During operation, the battery performs two primary functions: it acts as a load during charging and as a generator during discharging. The charging and discharging processes can be represented using Equations (5) and (6) (Danang *et al.*, 2018).
Charging Process:

$$E_B(t) = E_B(t-1) * (1-\sigma) + (E_G(t) - \frac{E_L(t)}{\eta_{inv}}) * \eta_B\,(t) \tag{5}$$

Discharging Process:

$$E_B(t) = E_B(t-1) * (1-\sigma) - \left(\frac{E_L(t)}{\eta_{inv}} - E_G(t)\right) \tag{6}$$

3.3.4 Biodiesel Generator

The power generated by a diesel generator must exceed the peak load. The hourly fuel consumption cost (C_F) of the diesel generator can be expressed using Equation (7) (Charadi et al., 2023).

$$C_F \;=\; P_{fuel} \,.\, F_{GBD} \tag{7}$$

Where $\boldsymbol{P_{fuel}}$ represents the fuel price based on market rates, and $\boldsymbol{F_{GBD}}$is the fuel consumption of the diesel generator (liters per hour). According to manufacturer recommendations, the maximum output power of a diesel generator is limited to 85% of its rated capacity.

3.3.5 Power Flow Management Strategy

The flowchart of the proposed power flow in the hybrid microgrid system is shown in Fig. 3. The power supply operation is divided into two modes: (i) when the power generated by the solar PV and wind turbines exceeds the load demand, and (ii) when the power generated by the solar PV and wind turbines is insufficient to meet the total load demand. In mode (i), the excess generated power is used to charge the battery until the maximum state of charge (SoC_{max}) is reached.

The power flow in this condition can be expressed by Equation (8).

$$P_{load}(t)x\ \Delta t = ((P_{PV}(t) + P_{WT}) - E_{CH}(t))x\Delta t\ x\ \eta_{inv}\ (t) \quad (8)$$

If the battery state of charge reaches its maximum limit (SoC_{max}), the excess power is diverted to the dummy load (P_{dummy}), as expressed in Equation (9).

$$P_{dum}(t)x\ \Delta t = ((P_{PV}(t) + P_{WT})\ \Delta t\ \eta_{inv} - P_{load}(t) - E_{CH}(t) \quad (9)$$

In mode (ii), when the power generated by the solar PV and wind turbines is lower than the load demand and the battery state of charge is above the minimum limit (SoC_{min}), the battery operates in discharge mode. The corresponding power flow is expressed by Equation (10).

$$P_{load}(t)x\ \Delta t = ((P_{PV}(t) + P_{WT}(t) + E_{DIS}(t))\Delta t\ \eta_{inv}\ (t) \quad (10)$$

If the combined power generated by the solar PV, wind turbines, and battery is insufficient to meet the load demand, the power deficit is supplied by the diesel generator, as expressed in Equation (11).

$$P_{DG}(t)x\ \Delta t = P_{load} - ((P_{PV}(t) + P_{WT}(t) + E_{DIS}(t))\quad \Delta t\ \ \eta_{inv}\ (t) \quad (11)$$

3.4 Formulation of Multi-Objective Optimization Functions

The Hybrid COA–WCA optimization algorithm is designed to minimize three conflicting objectives, namely the Cost of Energy (COE), Loss of Power Supply Probability (LPSP), and Dummy Load (DL). These objectives are essential for achieving both operational efficiency and long-term system sustainability. To address the multi-objective nature of the problem, the Weighted Sum Method (WSM) is employed. This approach transforms multiple objective functions, including COE, LPSP, and DL, into a single aggregated objective function, allowing the problem to be solved using a single optimization framework (Guo-ping et al., 2020; Petrelli et al., 2021; Salehi et al., 2022). Mathematically, the aggregated objective function (F_{agg}) is expressed as:

$$F(x) = w_1 \cdot f_1(x) + w_2 \cdot f_2(x) + w_3 \cdot f_3(x) \quad (12)$$

This objective function is subject to the constraint $w_1 + w_2 + w_3 = 1$, where each weight $w_i > 0$. The Weighted Sum Method (WSM) is adopted due to its simplicity, flexibility, and effectiveness in transforming multi-objective problems into scalar optimization models. In this approach, multiple optimization runs are performed by assigning different combinations of weights w_1, w_2, and w_3 to identify the most appropriate aggregated objective value (Alhawsawi, Salhein and Zohdy, 2024). WSM enables the management of trade-offs between cost and reliability and is well suited for real-world microgrid applications. In this study, the selected weights are $w_1 = 0.40$, $w_2 = 0.57$, and $w_3 = 0.03$.

These weights represent preference parameters used to transform the multi-objective problem into a single aggregated objective function, rather than values selected arbitrarily. Specifically, LPSP (0.57) is assigned the highest weight because this study emphasizes system operation and design under uncertainty therefore, service continuity and supply reliability are considered dominant requirements. COE (0.40) is assigned the second highest weight as an indicator of long-term economic efficiency, particularly to differentiate among technically feasible solutions. Meanwhile, DL (0.03) is given a relatively small weight, as it functions as an additional penalty term compared to the two primary criteria. For comparison, Diab 2019 (Diab *et al.*, 2019), used weighting values of 0.400, 0.599, and 0.001, for w_1, w_2, and w_3 respectively.

3.4.1 Parameter Optimization

The three parameters that serve as multi-purpose sizing optimization objectives for this hybrid microgrid system are to minimize loss of power supply probability (LPSP), cost of energy (COE), and dummy load (L_{dum}), using the weight sum method (WSM) approach.

3.4.1.1 Loss of Power Supply Probability (LPSP)

The Loss of Power Supply Probability (LPSP) is a widely used indicator for evaluating the reliability of a microgrid system. LPSP is defined as the ratio of the total energy deficit to the total load over a specified study period $\boldsymbol{T}$, which is typically one year. The LPSP can be evaluated at any time step $\boldsymbol{t}$ within the study period (Diab *et al.*, 2019; Mokhtara *et al.*, 2021; Belboul *et al.*, 2022). An LPSP value of 1 indicates that the load demand cannot be fully met, whereas a value of 0 indicates that the load is completely satisfied. The LPSP is formulated as shown in Equation (13).

$$\boldsymbol{LPSP} = \frac{\sum_0^T (\boldsymbol{P_L(t)} - [\boldsymbol{P_{PV}(t)} + \boldsymbol{P_{WT}(t)}] + \boldsymbol{P_{Bat(t-1)}} + \boldsymbol{P_{DG(t)}})}{\sum_{t=1}^{T} \boldsymbol{P_L(t)}} \quad (13)$$

Where LPSP, $\boldsymbol{P_L(t)}$, $\boldsymbol{P_{PV}(t)}$, $\boldsymbol{P_{WT}(t)}$, $\boldsymbol{P_{DG}(t)}$, $\boldsymbol{P_{Batt}(t-1)}$, and $\boldsymbol{T}$ denote, respectively, the Loss of Power Supply Probability, the load power at time $\boldsymbol{t}$, the solar PV power generated at time $\boldsymbol{t}$, the wind turbine power generated at time $\boldsymbol{t}$, the diesel generator power generated at time $\boldsymbol{t}$, the battery power stored at time $\boldsymbol{t-1}$, and the study period of the microgrid system, which is one year (8760 hours) in this study.

In this study, the loss of power supply is treated as a constraint in the optimization process. To ensure a 100% renewable energy microgrid system, a target LPSP value ($\boldsymbol{\varepsilon}_{LPSP}$) must be predefined. According to Diab et al. (2020), the acceptable value of $\boldsymbol{\varepsilon}_{LPSP}$is set to 0.04. Furthermore, the reliability constraint associated with the LPSP can be formulated using Equation (14), which is enforced throughout the optimization process.

$$LPSP \leq \varepsilon\ LPSP \quad (14)$$

Where $\varepsilon LPSP$ represents the required reliability level, which is set to a value below 4%.

3.4.1.2 Cost of Energy (COE)

One of the primary economic objectives of the optimization process is to minimize the Cost of Energy (COE). COE represents the total cost required to generate electrical energy, expressed in USD/kWh. To calculate the COE, both the total

system cost and the total electrical energy supplied to the load over a given period must be determined. In this study, the evaluation period is one year. The total cost of a hybrid microgrid system includes the initial investment cost (capital cost), operation and maintenance costs ($\boldsymbol{C_{O\&M}}$), and equipment replacement costs ($\boldsymbol{C_{rep}}$). The annual total cost ($\boldsymbol{C_{ann\_T}}$) used for COE calculation is derived using the annualized net present value approach and is expressed by Equation (15).

$$C_{ann\_T} = C_{ann\_cap} + C_{ann\_o\&m} + C_{ann\_rep} \quad (15)$$

Where C_{ann_cap}, $C_{ann\_o\&m}$, and C_{ann_rep} denote, respectively, the annualized capital cost, the annual operation and maintenance cost, and the annual equipment replacement cost. In economic calculations, all investment costs are converted into equivalent annual costs using the Capital Recovery Factor (CRF). The CRF is calculated using the following equation:

$$CRF_{(r,n)} = \frac{r(1+r)^n}{(1+r)^n - 1} \quad (16)$$

Where CRF, r, and n denote, respectively, the Capital Recovery Factor, the interest rate, and the system lifetime in years. Finally, the Cost of Energy (COE) can be calculated using the following equation:

$$COE = \frac{C_{ann\_tot}}{\sum_{h=1}^{h=8760} P_{load}} = \frac{NPC}{\sum_{h=1}^{h=8760} P_{load}} \; x \; CRF \quad (17)$$

Where COE, C_{ann_tot}, P_{load}, NPC, and CRF denote, respectively, the Cost of Energy (USD/kWh), the total annual cost of electricity generation (USD), the total electrical load served over one year (kWh), the Net Present Cost (USD), and the Capital Recovery Factor. A more detailed description of the total cost components of the microgrid system is provided in the following subsections.

a) Capital Cost

The capital cost of a microgrid system represents the total investment required for the planning and construction of the entire power generation system. In this study, the microgrid system consists of four main components: photovoltaic (PV) modules, wind turbines (WT), batteries (Bat), and diesel generators (DG). The annualized capital cost of each microgrid component can be expressed using the following equation:

$$\begin{cases} C_{ann\_cap\_PV} = C_{cap\_PV} \; x \; CRF \; (r, M_{PV}) \\ C_{ann\_cap\_WT} = C_{cap\_WT} \; x \; CRF \; (r, M_{WT}) \\ C_{ann\_cap\_Bat} = C \; x \; CRF \; (r, M_{Bat}) \\ C_{ann\_cap\_DG} = C \; x \; CRF \; (r, M_{DG}) \end{cases} \quad (18)$$

Where $C_{ann\_cap\_PV}$, $C_{ann\_cap\_WT}$, $C_{ann\_cap\_Bat}$, and $C_{ann\_cap\_DG}$ represent, respectively, the annualized capital costs of the solar PV, wind turbine, battery, and diesel generator.

$$C_{ann\_cap} = C_{ann\_cap\_PV} + C_{ann\_cap\_WT} + C_{ann\_cap\_Bat} + C_{ann\_cap\_DG} \quad (19)$$

b) Annual Operation and Maintenance Costs

The annual operation and maintenance (O&M) costs of the microgrid system can be formulated as follows:

$$C_{ann\_o\&m} = C_{ann\_o\&p\_PV} + C_{ann\_o\&m\_WT} + C_{ann\_o\&m\_Bat} + B_{ann\_o\&m\_DG} \quad (20)$$

Where $C_{ann\_o\&m\_PV}$, $C_{ann\_o\&m\_WT}$, $C_{ann\_o\&m\_Bat}$, and $C_{ann\_o\&m\_BDG}$ denote, respectively, the annual operation and maintenance costs of the solar PV, wind turbine, battery, and biodiesel generator.

c) Annual Equipment Replacement Costs

During operation, each component of a microgrid system is subject to aging and potential failure. To ensure continuous and reliable power generation, equipment replacement costs must be considered. The present value of the equipment replacement cost for the microgrid system (C_{rep}) can be calculated using the following equation:

$$C_{ann\_rep} = \sum_{j=1}^{n_{rep}} Kc_{rep} \; C_u \; \left(\frac{1+i}{1+r}\right)^{nj/n_{rep}+1} \quad (21)$$

Where $K_{c,rep}$, C_u, i, n_{rep}, n_j, and $\boldsymbol{r}$denote, respectively, the number of system units to be replaced, the replacement cost per unit (USD), the equipment replacement inflation rate (%), the number of replacements over the project lifetime, the project lifetime (years), and the interest rate (%).

3.4.1.3 Dummy Load (DL)

The dummy load absorbs excess power when the energy generated by the PV and wind turbines exceeds the load demand and the battery has reached its maximum capacity. This mechanism prevents battery overcharging and helps maintain system stability. In this study, minimizing the dummy load is considered the third objective function, together with COE and LPSP. Mathematically, the power absorbed by the dummy load is expressed in Equation (9), which indicates that excess energy is diverted to the dummy load only after the load demand and storage requirements have been fully satisfied.

3.4.2 Constraint

In the hybrid microgrid system, each component operates under a set of constraints that must be satisfied to ensure reliable and optimal performance. The primary constraint is the power balance condition, which requires that the total power generated by all sources at time t, including solar PV $P_{PV}(t)$, wind turbines $P_{WT}(t)$, batteries $P_{Bat}(t)$, and diesel generators $P_{DG}(t)$, must be equal to the load demand $P_L(t)$, as expressed in Equation (22). In addition, the power supplied by the diesel generator at any time must not exceed its rated capacity P_{DG_rated}, as defined in Equation (23). To prevent battery overcharging and excessive discharging, the state of charge (SoC) of the battery bank is constrained within predefined limits throughout the operation period, as described in Equations (24) and (25). Specifically, the maximum state of charge (SoC_{max}) represents the full battery capacity, while the minimum state of charge (SoC_{min}) corresponds to the allowable depth of discharge. Furthermore, to ensure system reliability, the Loss of Power Supply Probability (LPSP) must remain below the specified reliability threshold β_L, as given in Equation (26). In this study, the value of $\beta_L$is set to be less than 0.04. The complete set of constraints applied in this study is summarized in the following equation.

$$P_{PV}(t) + P_{WT}(t) + P_{BAT}(t) + P_{DG}(t) = P_L(t) \quad (22)$$

$$P_{DG}(t) \leq P_{DG\_rated}(t) \quad (23)$$

$$SoC_{min} \leq SoC(t) \leq SoC_{max} \quad (24)$$

$$SoC(t+1) = SoC(t)(1-\sigma) \quad (25)$$

Algorithm 1. Pseudocode of COA

```
Initialize the coyote population within the search-space bounds and partition it into N_p packs..
Evaluate the fitness of all coyotes.
Set t = 0 and determine the initial global best solution x*.
while (t < T_max and the stopping criterion is not satisfied) do
    for each pack p = 1, 2, ..., N_p do
        Determine the alpha coyote α^{p,t} in pack p.
        Compute the social tendency cult^{p,t} of pack p.
        for each coyote c in pack p do
            Randomly select cr1 and cr2 from the same pack.
            Compute:
              δ_1 = α^{p,t} - soc_{cr1}^{p,t}, and
              δ_2 = cult^{p,t} - soc_{cr2}^{p,t}.
            Update the social condition to obtain new_soc_c^{p,t}.
            Evaluate the fitness of new_soc_c^{p,t}.
            if new_soc_c^{p,t} is better than soc_c^{p,t} then
                Replace soc_c^{p,t} with new_soc_c^{p,t}.
            end if
        end for
        Perform following actions:
          pup generation,
          birth-death replacement, and
          age updating.
    end for
    Allow coyote migration between packs with probability P_e.
    Update the global best solution x*.
    t = t + 1
end while
Return x* as the best solution
```

$$LPSP \leq \beta_L \tag{26}$$

3.5 Optimization Algorithm Approach

This section provides a detailed description of the optimization methods employed in this study, including COA, WCA, WOA, as well as the proposed hybrid COA–WCA approach.

3.5.1 Coyote Optimization Algorithm (COA)

The Coyote Optimization Algorithm (COA) is a population-based metaheuristic introduced by Pierezan and Coelho (2018), inspired by the social behavior of coyote packs (Canis latrans) (Pierezan and Dos Santos Coelho, 2018). In this algorithm, the population is divided into several packs, where each coyote represents a candidate solution in the search space. The adaptation level of each coyote is evaluated using the objective function, while the best-adapted coyote in each pack is identified as the alpha coyote. In addition, the social tendency of each pack is determined to represent the collective behavioral pattern of the group.

The optimization process is mainly guided by the influence of the alpha coyote and the pack's social tendency, which are used to update the position of each coyote. This mechanism enables COA to balance exploitation around promising solutions and exploration across the search space. To preserve population diversity and reduce the risk of premature convergence, COA incorporates biological mechanisms, including birth, death, aging, and transition among packs. Through these adaptive and cooperative processes, COA is suitable for solving complex, nonlinear, and multidimensional optimization problems. For clarity, the pseudocode of the Coyote Optimization Algorithm (COA) is presented in Algorithm 1.

3.5.2 Water Cycle Algorithm (WCA)

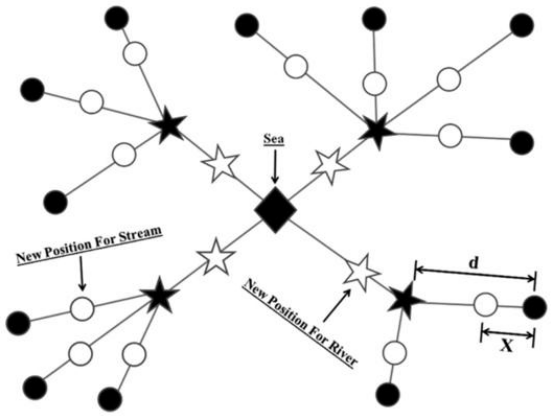

Fig. 4 Schematic representation of the movement of WCA towards the optimal solution (Eskandar, H. *et al.*2012).

The Water Cycle Algorithm (WCA), developed by Eskandar et al. (2012), is a population-based metaheuristic optimization method inspired by natural hydrological processes, including stream flow, river formation, rainfall, and evaporation. In WCA, each candidate solution is represented as a raindrop or stream, while the best solution is assigned as the sea, which acts as the main attractor in the search process. Several high-quality solutions are selected as rivers, and the remaining streams move either toward the rivers or directly toward the sea. This

Algorithm 2. Pseudocode of WCA

```
Initialize N_pop candidate solutions X_i randomly within the search-space bounds.
Evaluate the objective value of each candidate solution.
Sort the population according to the objective value.
Assign the best solution as the sea X_sea, and
select the next best solutions as rivers.
Assign the remaining solutions as streams connected to rivers or directly to the sea.
Set iter = 1.
while (iter <= MaxIter) do
    for each stream do
        if the stream is connected directly to the sea then
            Update the stream position toward X_sea.
        else
            Update the stream position toward its assigned river.
        end if
    end for
    for each river do
        Update the river position toward X_sea.
    end for
    Evaluate the updated population.
    Exchange positions if:
      a stream becomes better than its river, or
      a river becomes better than the sea.
    Check the evaporation condition around the sea.
    if the evaporation condition is satisfied then
        Generate new streams using the rain process, and
        reassign their connections.
        Evaluate the new streams.
    end if
    Update d_max, if required.
    Update X_sea as the current best solution.
    iter = iter + 1
end while
Return X_sea as the best solution
```

hierarchical stream–river–sea mechanism enables WCA to iteratively improve solution quality while maintaining a balance between global exploration and local exploitation.

The WCA procedure begins with random population initialization, followed by objective function evaluation and classification of solutions into sea, rivers, and streams. The flow intensity is then determined to assign streams to the corresponding rivers or directly to the sea, after which their positions are updated through the flow mechanism. If a stream or river obtains a better objective value, role exchange is performed to update the current best solution. To prevent premature convergence, WCA incorporates evaporation and raining mechanisms, where evaporation is triggered when the distance between a river and the sea becomes smaller than a predefined threshold (dmax). The subsequent raining process generates new streams to restore population diversity and reduce the risk of local optimum entrapment. Fig. 4 illustrates the schematic movement of WCA toward the optimal solution.

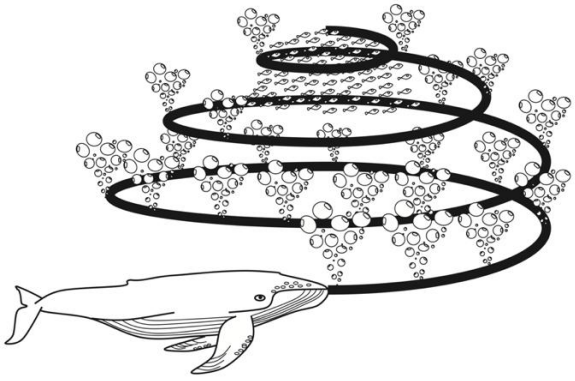

Fig. 5 Bubble-net feeding behavior of humpback whales . (Mirjalili, S. and Lewis, A. 2016)

Algorithm 3. Pseudocode of WOA

```
Initialize the whale population X_i (i = 1, 2, ..., N).
Set t = 0 and initialize the algorithm parameters a, A, C, l, and p.
Evaluate the fitness of each whale.
Determine the best search agent X*.
while (t < MaxIter) do
    Update a, A, C, l, and p.
    for each whale X_i do
        if p < 0.5 then
            if |A| < 1 then
                Update X_i using the encircling mechanism around X*.
            else
                Select a random whale X_rand.
                Update X_i using the exploration mechanism around
                X_rand.
            end if
        else
            Update X_i using the spiral position-updating mechanism around X*.
        end if
    end for
    Evaluate the updated population.
    Update X* if a better solution is found.
    t = t + 1
end while
Return X* as the best solution
```

For clarity, the pseudocode of the Water Cycle Algorithm (WCA) is presented in Algorithm 2.

3.5.3 Whale Optimization Algorithm (WOA)

The Whale Optimization Algorithm (WOA) is a population-based metaheuristic optimization method introduced by Mirjalili and Lewis, inspired by the bubble-net hunting behavior of humpback whales. In WOA, each whale represents a candidate solution, while the best solution obtained so far is considered the prey or the approximate global optimum. The algorithm begins by randomly initializing the population within the predefined search bounds, evaluating the fitness of each candidate solution, and identifying the best search agent. During the iterative process, the position of each whale is updated through encircling prey, bubble-net attacking, and searching for prey mechanisms. In nature, humpback whales encircle prey near the water surface while generating spiral-shaped bubble trails, as illustrated in Fig. 5.

The encircling and bubble-net mechanisms support the exploitation phase by guiding search agents toward the best solution through shrinking encircling and spiral movement strategies. Meanwhile, the search-for-prey mechanism enhances exploration by allowing agents to update their positions relative to randomly selected whales, thereby improving population diversity and reducing premature convergence. The balance between exploration and exploitation is controlled by an adaptive parameter that decreases linearly from 2 to 0 throughout the iterations. The process continues until the stopping criterion is satisfied, and the best solution obtained is selected as the optimal solution. For clarity, the pseudocode of the Whale Optimization Algorithm (WOA) is presented in Algorithm 3

3.5.4 Proposed Hybrid COA-WCA Algorithm

These two algorithms exhibit complementary characteristics: COA excels in adaptive local search (exploitation), while WCA is effective in global search (exploration). Therefore, the combination of COA and WCA presents a promising approach for overcoming the limitations of each individual algorithm and enhancing global search efficiency in complex microgrid optimization problems (Cetinbas et al., 2022; Charadi et al., 2023).

This research proposes a hybrid metaheuristic that combines the global exploration ability of the Coyote Optimization Algorithm (COA) with the strong local exploitation mechanism of the Water Cycle Algorithm (WCA) to address the multi-objective optimization of a hybrid renewable microgrid. The hybridization aims to improve convergence stability and solution quality by using COA to locate promising regions of the search space and WCA to intensively refine the best region identified.

As shown in the flow diagram Fig. 6, the procedure consists of three stages. First, the decision-variable bounds, objective functions, constraints, and algorithmic parameters are initialized. COA is then executed using a randomly generated population of candidate microgrid configurations. At each iteration, solutions are updated according to COA's social adaptation mechanism and evaluated using the defined multi-objective formulation. The best solution obtained at the end of this phase is stored as Best_pos_COA with its associated performance value Best_score_COA. Second, the WCA population is initialized using Best_pos_COA to ensure that the exploitation phase starts from a high-quality reference solution while maintaining local diversity. The WCA population is

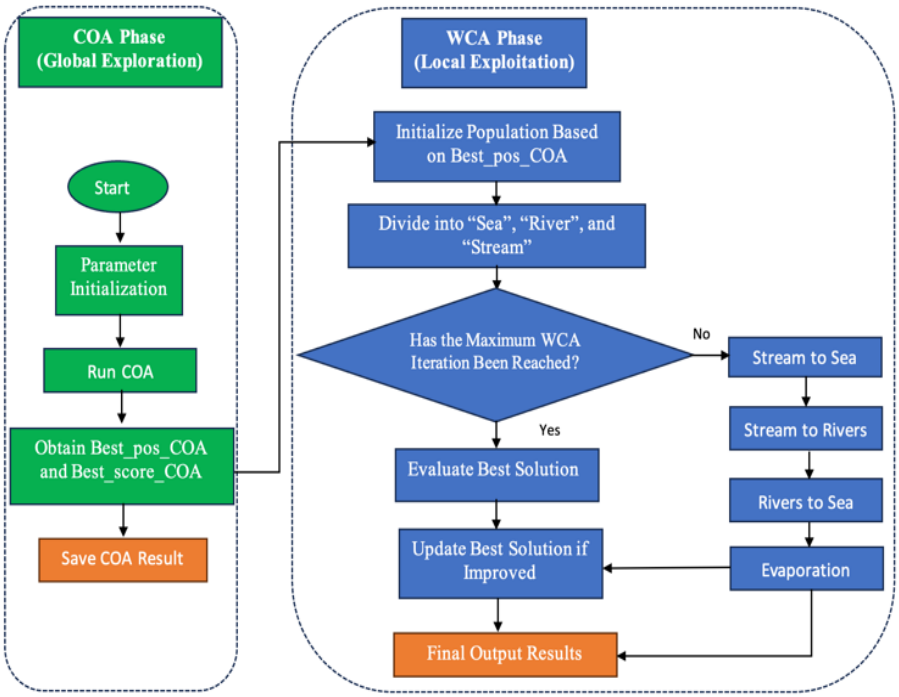

Fig. 6 Flow diagram Hybrid Algorithm COA-WCA

Table 1
Technical and economic character hybrid microgrid component

Component	Parameter	Value
Solar PV (LR6-72)	Nominal Max. Power	330 W
	Module efficiency	17%
	Open circuit voltage	46.1V
	Short circuit current	8.88 A
	Temperature coefficient at max power	− 0.41%/°C
	Battery performance ratio	80%
	Initial cost (total)	320$
	O & M annual cost	4.8$
	Replacement cost	256.7$
Wind Turbine M2-2-1000	Rated power	1000 W
	Rated voltage	24/48/96 V
	Cut-in win speed	2.5 m/s
	Rated wind speed	12 m/s
	Cut-out win speed	25 m/s
	Safe windspeed	50< m/s
	Initial cost (total)	812 $
	O & M cost annual	12$
	Replacement cost	650$
Battery LMFP	Nominal capacity	270 Ah
	Nominal voltage	12V
	Design lifetime	7year
	Initial cost (total)	730 $
	O & M cost	11$
	Replacement cost	604$
Diesel generator MU3000(S)-1	Rated Power	3000 kVA
	Power rating	2400 kW
	Rated voltage	400/230 V
	Fuel consumption 110% load	644 l/h
	Fuel consumption 100% load	585 l/h
	Fuel consumption 75% load	438.7 l/h
	Fuel consumption 50% load	292.5 l/h
	Initial cost total	289,730 $
	O & M cost annual	4,346 $
	Replacement cost	231,784 $

hierarchically classified into Sea (best solution), Rivers (next best solutions), and Streams (remaining candidates). Third, WCA performs local refinement through directed flow operations, where Streams move toward Rivers and the Sea, and Rivers move toward the Sea. After each movement, candidate feasibility is enforced and objective values are re-evaluated, the best solution is updated whenever an improvement is found. To prevent stagnation and premature convergence, an evaporation mechanism is applied to re-distribute part of the population when diversity becomes insufficient. The refinement continues until the stopping criterion (e.g., maximum WCA iterations) is satisfied, and the final best solution(s) are reported as the optimized microgrid configuration under the multi-objective criteria.

Four optimization algorithms, namely COA, WCA, WOA, and the proposed Hybrid COA-WCA, were implemented and evaluated through simulations using MATLAB, based on real operational data from Nusa Penida Island. The dataset includes electrical load profiles, solar irradiance, ambient temperature, and wind speed. The simulations were conducted over one year of operation, corresponding to 8,760 hours. The technical and economic characteristics of the hybrid microgrid system components are summarized in Table 1. The lifetime of the hybrid microgrid system is assumed to be 25 years, with an interest rate of 5%. The technical and economic modeling required for the optimization process is formulated using Equations (1)–(21). The energy management strategy of the hybrid microgrid system follows the power flow logic illustrated in Fig. 3. To simplify the multi-objective optimization problem, the Weighted Sum Method (WSM) is employed, as formulated in Equation (12). The optimization constraints applied in this study are defined by Equations (22)–(26).

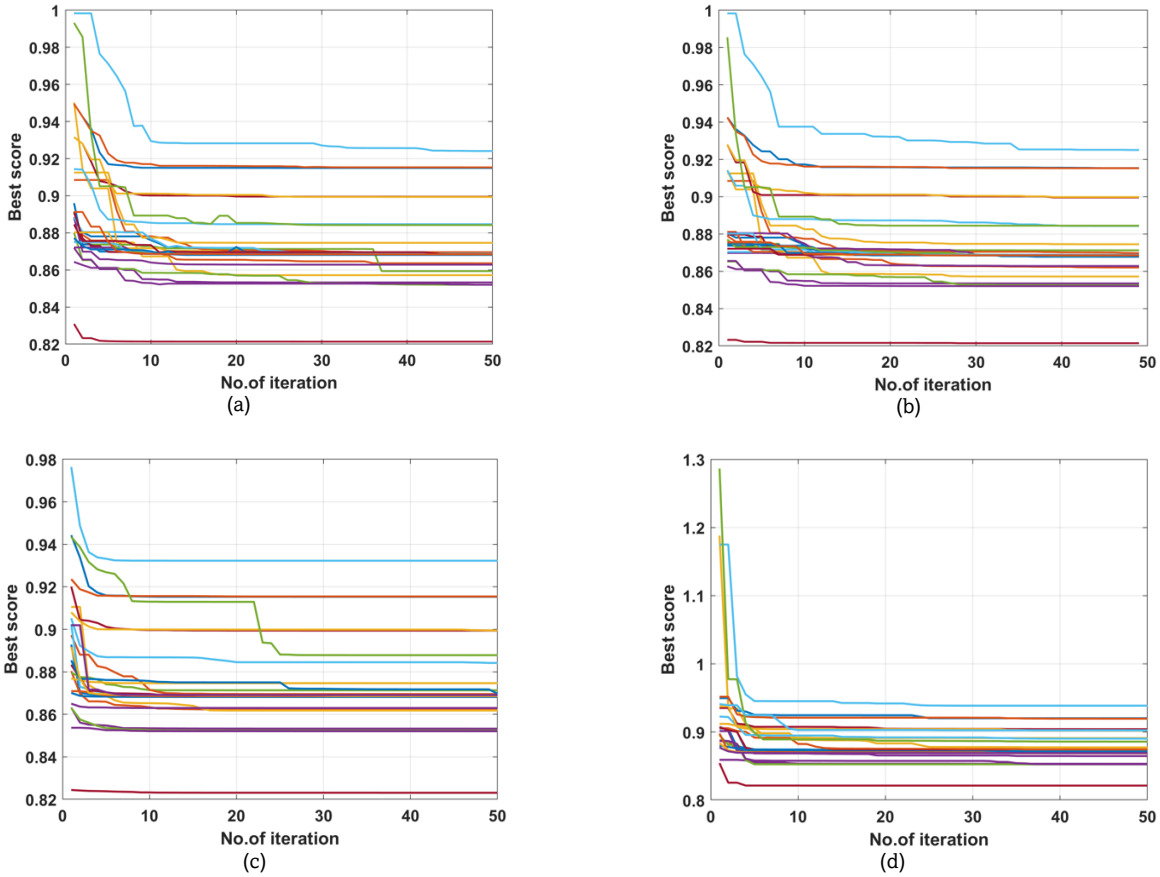

Fig. 7 Convergency curves of robustness test in 30 uncertainty condition, (a) Hybrid COA-WCA, (b) COA, (c) WCA and (d) WOA)

4. Result and Discussion

This section presents the results and discussion based on the simulation experiments conducted in this study. For clarity and systematic presentation, the section is organized into seven subsections. Experimental Simulation Scenario describes the experimental setup and parameter settings used in the study. Sensitivity Analysis examines the influence of key parameters on system performance. Convergence Behavior analyzes the stability and convergence characteristics of the applied method. Descriptive Performance Statistics summarizes the main statistical indicators representing system performance. Pareto Front Visualization presents the trade-offs among the optimization objectives. Power Supply and Load Balancing discusses the distribution of energy resources and the load balancing performance of the system. Finally, Implications and Future Research Directions outlines the implications of the findings and potential directions for future work.

4.1 Experimental Simulation Scenario

This section presents the experimental simulation scenario used to evaluate the performance of the Hybrid COA-WCA algorithm in optimizing component sizing for a renewable energy-based hybrid microgrid system. The performance of the proposed Hybrid COA-WCA algorithm is compared with that of other optimization methods, including COA, WCA, and WOA, through a series of simulations conducted across 30 experimental scenarios with varying parameter settings.

The 30 experimental scenarios (representing possible uncertain operating conditions and population parameter variations) simulated in this study can be broadly categorized into four groups:

1) Population parameter variations (11 scenarios). For COA, the number of coyote packs (N_p) and the number of coyotes per pack (N_c) were randomly varied from the minimum configuration of $N_p = 4$, $N_c = 4$to the maximum configuration of $N_p = 15$, $N_c = 8$. For WCA, the population size (N_{pop}) and the number of streams (N_{sr}) were randomly varied from the minimum configuration of $N_{pop} = 15$, $N_{sr} = 4$to the maximum configuration of $N_{pop} = 50$, $N_{sr} = 10$. For WOA, the number of search agents was varied from 5 to 55 with an interval of 5.
2) Electrical load variations (5 scenarios). The load demand was adjusted from a 5% decrease to a 20% increase relative to the nominal condition, with a 5% interval.
3) Weather condition variations. These include changes in solar irradiation, ambient temperature, and wind speed, each evaluated under two scenarios: a 5% decrease and a 5% increase relative to the nominal condition.
4) Generation unit cost and fuel price variations (4 scenarios each). These parameters were tested under scenarios ranging from a 5% decrease to a 15% increase relative to the nominal values, with a 5% interval.

4.2 Sensitivity Analysis

To evaluate the robustness of the Hybrid COA-WCA algorithm, a sensitivity analysis was conducted using 30 distinct experimental scenarios, as described in Section 4.1. The performance of each algorithm was assessed by comparing its convergence behavior under these uncertain conditions. The

Table 2.
Results of the Robustness Test of the Algorithm

Criteria		Hybrid COA-WCA	COA	WCA	WOA
Number of Trials		30	30	30	30
Maximum Number of Iterations		50	50	50	50
Iterations Required to	Fastest	19	20	**11**	14
Reach Convergence	Latest	50	50	50	50
	Average	37	44	**31**	41
Iteration start value	Lowest	0.8309	**0.8234**	0.8244	0.8544
	Highest	0.9983	0.9983	0.9764	**1.2865**
	Average	**0.9001**	0.9009	0.8934	0.9302

convergence criteria and results for all algorithms are presented in Table 2 and Fig. 7.

Based on the convergence curves obtained from the robustness tests across the 30 uncertainty scenarios, the Hybrid COA-WCA algorithm exhibits the most consistent and efficient performance. The curves show a sharp decrease in the objective function during the initial iterations (approximately iterations 1–5), followed by rapid stabilization before iteration 15. In the final stage, the values remain within a relatively narrow range (approximately 0.85–0.92), with minimal fluctuation. This behavior indicates that the hybridization strategy effectively balances global exploration and local exploitation, leading to faster convergence and improved stability under varying uncertainty conditions.

For COA, the convergence curves exhibit a marked decline in the objective function during the early iterations (approximately iterations 1–10), reflecting its strong global exploration capability in identifying promising search regions. As the iterations proceed, however, the rate of convergence becomes more gradual. Although some variation in initial performance is observed across different scenarios, most curves eventually stabilize within a relatively narrow range (approximately 0.85–0.92) without significant oscillations in the later iterations. This indicates that COA provides stable and reasonably robust performance, although its convergence rate is slower than that of the hybrid method under certain conditions.

WCA also exhibits a rapid decline in objective function values during the early iterations (approximately iterations 1–5). However, in several scenarios, additional iterations (approximately 20–30) are required to reach a stable state. In the final stages, the objective values converge within a relatively narrow range of approximately 0.85–0.90, indicating good stability with minimal oscillations. These results indicate that WCA is robust under uncertainty, although its convergence is generally more gradual and requires more iterations to achieve stabilization.

Similarly, WOA exhibits rapid convergence during the initial iterations (approximately iterations 1–5), followed by stabilization between iterations 10 and 20. For most scenarios, the objective values converge within a relatively narrow range of approximately 0.85–0.92, with limited fluctuations in the final stage, indicating consistent adaptability under the uncertainty scenarios. However, some variation in the final solution quality is still observed, indicating that WOA performs well but with slightly lower consistency than the other algorithms.

All four algorithms exhibit stable convergence behavior under the robustness tests. However, the Hybrid COA–WCA outperforms the individual algorithms in terms of convergence speed, stabilization time, and performance consistency across the uncertainty scenarios. These findings indicate that the Hybrid COA–WCA approach is more suitable for solving optimization problems under highly uncertain conditions than COA, WCA, and WOA when applied individually.

At the final iteration (Table 3), the Hybrid COA–WCA achieves the lowest objective function value of 0.87258, followed by COA with 0.87303, WCA with 0.87367, and WOA with 0.87756. These results indicate that, although the Hybrid COA–WCA algorithm requires slightly more iterations, it consistently produces lower objective function values, reflecting better solution quality.

Furthermore, the Hybrid COA–WCA algorithm exhibits the smallest fluctuation in objective function values at the final iteration, ranging from a minimum of 0.82136 to a maximum of 0.92409. This is followed by COA (minimum: 0.82145, maximum: 0.92506), WCA (minimum: 0.82307, maximum: 0.93227), and WOA (minimum: 0.82137, maximum: 0.93860). The smaller fluctuation observed for Hybrid COA–WCA indicates greater stability and consistency in achieving optimal solutions across different experimental conditions.

Robustness testing across 30 uncertainty scenarios further highlights that faster convergence does not necessarily lead to superior final solutions. WCA reaches convergence the fastest (iteration 11), followed by WOA (iteration 14), while Hybrid COA–WCA and COA achieve their fastest convergence at iterations 19 and 20, respectively. Despite the slightly later convergence, Hybrid COA–WCA consistently outperforms the other algorithms by achieving the best final objective function value (0.87258), followed by COA (0.87303) and WCA (0.87367), whereas WOA yields the least favorable result (0.87756). The mean convergence trajectory also shows that Hybrid COA–WCA undergoes a sharp reduction in the objective function during the early iterations and stabilizes rapidly, indicating its ability to effectively explore promising search regions while maintaining efficient exploitation until convergence.

The sensitivity analysis conducted across the 30 experimental scenarios further confirms that the Hybrid COA–WCA algorithm exhibits greater stability and faster convergence than the individual algorithms (COA, WCA, and WOA), in the context of hybrid microgrid design and renewable energy systems. The rapid initial convergence of Hybrid COA–WCA, resulting from the integration of COA's global search mechanism and WCA's local exploitation capability, enables the algorithm to approach optimal solutions more efficiently while maintaining stability under a wide range of uncertainty conditions. These results are consistent with previous studies on hybrid algorithms, such as HHO–EO and ICA–PSO, which also reported improved convergence stability in uncertain environments (Kharrich *et al.,* 2021; Çetinbaş *et al.,* 2022; Ebrahim *et al.,* 2024). Therefore, Hybrid COA–WCA demonstrates robust performance in handling input variations and further highlights the advantage of hybrid approaches in maintaining solution stability under uncertainty.

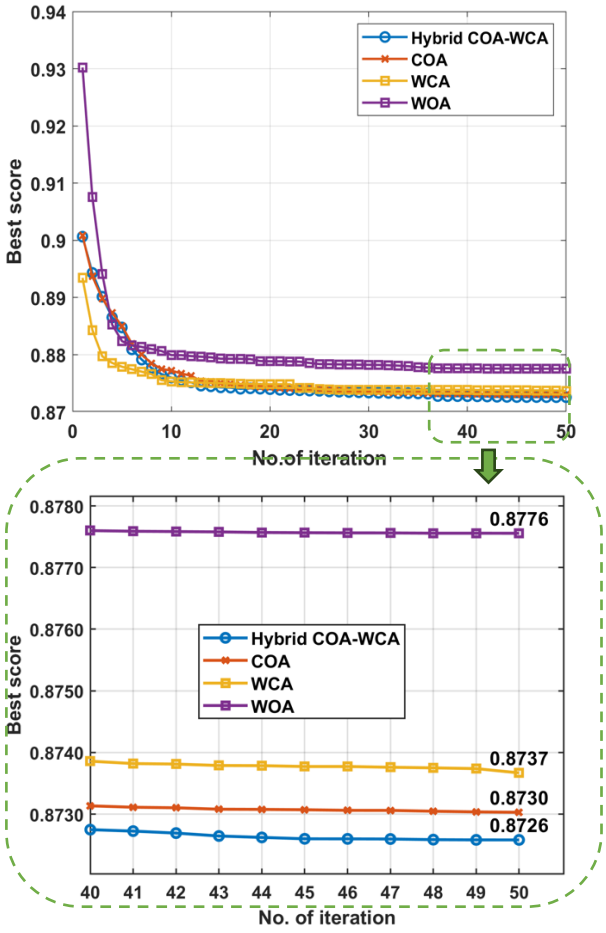

Fig. 8 Comparison Convergence Curve (Hybrid COA-WCA, WCA dan WOA)

4.3 Convergence Behavior

The convergence behavior of the optimization algorithms was examined by comparing their average convergence curves, as shown in Fig. 8. The figure presents the convergence trends of the COA, WCA, WOA, and Hybrid COA–WCA algorithms from iteration 1 to iteration 50. The data were obtained by calculating the average objective function value at each iteration across 30 experimental scenarios, each representing different uncertainty conditions and population parameter variations, as described in Section 4.1. Therefore, the curves in Fig. 8 reflect the average performance of each algorithm under these diverse experimental conditions.

The Hybrid COA–WCA algorithm demonstrates the most stable and consistent convergence, with the objective function decreasing from 0.90064 at the initial iteration to 0.87258 at convergence. This smooth and monotonic trend highlights its efficiency in steadily approaching optimal solutions without significant fluctuations, indicating its ability to maintain consistent performance, particularly under uncertainty in load demand and renewable energy source (RES) conditions.

The COA algorithm, starting with an objective function value of 0.90085, gradually decreases to 0.87303. However, its convergence rate is slower than that of the Hybrid COA–WCA algorithm, and it exhibits larger fluctuations during the optimization process, indicating lower stability. Similarly, the WCA algorithm begins with a value of 0.89342 and shows steady but slower convergence, reaching 0.87367. Although the final value is acceptable, its convergence stability is lower than that of the Hybrid COA–WCA and COA algorithms. The WOA algorithm, starting with a higher initial value of 0.93022, requires more iterations to approach the optimal solution and exhibits greater fluctuations, indicating less stable convergence than the other algorithms.

First data group in Table 3 presents the statistical dispersion measures of the best objective function value ($\boldsymbol{f}$) at iteration 50, including the mean, standard deviation, min, max, median, coefficient of variationcon (CV), confidence interval (C195), and interquartile range (IQR). Although the Hybrid COA–WCA yields the lowest objective function value at the final iteration (0.87258), while COA and WCA produce slightly higher values (0.87303 and 0.87367, respectively), the differences are marginal. These results indicate a numerical tendency favoring the hybrid approach however, the substantial overlap in the 95% confidence intervals (Hybrid: [0.86478; 0.88038], COA: [0.86524; 0.88082], WCA: [0.86571; 0.88163]) and the cross-scenario variability (SD ≈ 0.021) suggest that the performance differences are not statistically significant.

The findings of this study suggest that the Hybrid COA–WCA algorithm provides competitive and stable performance compared with the other algorithms under the evaluated conditions. The main advantage of the Hybrid COA–WCA lies in its greater convergence stability and more consistent solution quality, particularly in handling uncertainties related to load demand and renewable energy source (RES) availability. This observation is consistent with the findings of Diab et al. (2019), who reported that hybrid algorithms, although not always statistically superior, tend to provide more stable convergence and more reliable solutions under uncertain operating conditions.

A comparison with the literature further supports the view that hybrid algorithms in microgrid (MG) design and hybrid renewable energy system (HRES) optimization often exhibit stronger and more stable convergence than single algorithms. For example, Çetinbaş *et al.* (2022) demonstrated that the combination of the Harris Hawks Optimizer (HHO) and the Arithmetic Optimization Algorithm (AOA) achieved better convergence and produced solutions closer to the optimum than either algorithm applied individually. Similarly, Arul et al. (2022) reported that the hybrid Grey Wolf Optimizer (OGGWO) generated a wider and more stable Pareto front in multi-objective microgrid scheduling. In addition, the integration of COA with other global exploration techniques, as reported by Ebrahim et al. (2024) and Çetinbaş et al. (2022), resulted in faster convergence toward better solutions than the use of COA or WCA alone. In terms of convergence stability, the Hybrid COA–WCA exhibits a smoother and more monotonic convergence pattern without significant fluctuations across iterations. This is consistent with the findings of Güven et al. (2023) and Çetinbaş *et al.* (2022), who suggested that hybrid algorithms can improve convergence stability, particularly in nonlinear and constrained optimization problems such as those encountered in MG/HRES design and scheduling.

This study also compares the Hybrid COA–WCA algorithm with COA, WCA, and WOA in terms of solution quality, robustness, and convergence behavior for energy system optimization. The Hybrid COA–WCA achieves the best overall performance, yielding the lowest mean objective function value (0.87274) and the smallest standard deviation, indicating the most consistent generation of high-quality solutions across multiple runs. In contrast, the WOA algorithm produces the

Table 3
Descriptive statistical performance of the optimization algorithm simulation results

Algorithm		Hybrid COA-WCA	COA	WCA	WOA
Best score objective function (f)	Mean	**0.87258**	0.87303	0.87367	0.87756
	StdDev	0.0208	**0.0208**	0.0213	0.0232
	Min	**0.82136**	0.82145	0.82307	0.82137
	Max	**0.92409**	0.92506	0.93227	0.93860
	Median	0.8684	0.8684	0.8686	0.8704
	CV	0.02392	**0.02388**	0.02438	0.02643
	C195%L	**0.86478**	0.86524	0.86571	0.8688
	C195%U	**0.88038**	0.88082	0.88163	0.8862
	IQR	0.0086	0.0057	**0.0055**	0.0204
COE	Average	1.388	1.384	1.382	**1.350**
	stdDev	0.039	**0.035**	0.047	0.045
LPSP	Average	**0.03180**	0.03202	0.03190	0.03272
	stdDev	0.00469	0.00476	0.00498	**0.00452**
DL	Average	6,609.0	6,409.5	6,458.6	**6,031.3**
	stdDev	1,361.9	**1,308.3**	1,326.3	1,914.1
N_PV (units)		63.413	62.815	64.546	**59.477**
N_WT (units)		35.903	35.881	35.389	35.776
N_Batt(units)		287	286	526	**284**
N_BDG(units)		2	2	2	2

highest mean objective value (0.87785) and the largest standard deviation, suggesting lower performance and greater variability.

These results are consistent with previous studies. Charadi et al. (2023) reported that a hybrid ICA–PSO strategy can improve operational efficiency and reduce costs in microgrid optimization, which is in line with the improved stability observed for the hybrid approach in this study. Similarly, Balasubramanyam and Sood (2023), through HFPSOMCS, highlighted improvements in convergence and stability for microgrid energy management, further supporting the robustness and stable convergence demonstrated by the Hybrid COA–WCA algorithm in this study paper.

4.4 Descriptive Performance Statistics

Table 3 summarizes the descriptive performance statistics of the four optimization algorithms based on 30 independent trials. The table presents three main groups of results: (1) the best objective function value ($\boldsymbol{f}$), (2) the multi-objective performance metrics, including Cost of Energy (COE), Loss of Power Supply Probability (LPSP), and Dummy Load (DL), and (3) the optimal number of units for the hybrid microgrid system components, namely solar PV modules (N-PV), wind turbines (N-WT), batteries (N-Batt), and biodiesel generators (N-BDG). Table 3 shows that the Hybrid COA-WCA algorithm performs well across several categories. Specifically, Hybrid COA-WCA achieves an average COE of 1.388, which is slightly higher than that of COA (1.384) and WCA (1.382), but higher than that of WOA (1.350). In terms of LPSP, Hybrid COA-WCA yields an average value of 0.03180, which is slightly lower than that obtained by COA (0.03202) and WOA (0.03272), but higher than the value produced by WCA (0.09130). For Dummy Load (DL), Hybrid COA-WCA results in an average value of 6,609.025, which is the highest among the compared algorithms, while WOA records a DL value of 6,031.288.

The optimization results for component sizing in the hybrid microgrid system indicate that the Hybrid COA-WCA algorithm produces a more balanced configuration, comprising 63,413 PV units, 35,903 wind turbine units, 287 battery units, and 2 biodiesel generator units. Compared with COA, the resulting configuration is largely comparable, with only minor differences in the number of components. Although WCA optimizes the number of PV units to a higher level (64,546 units), it requires a substantially larger number of battery units (526 units), indicating lower efficiency in optimizing storage capacity. In contrast, WOA produces a smaller number of PV units (59,477 units) while still maintaining a relatively balanced allocation between wind turbines and battery units.

4.5 Pareto Front Visualization

Fig. 9 presents the Pareto front visualization obtained from the multi-objective optimization process, illustrating the trade-offs among COE, LPSP, and DL. Fig. 9 was generated by applying min–max normalization (0–1 scaling) to the COE, LPSP, and DL values to allow a more appropriate interpretation. Min–max normalization across all combined solutions ensures that the comparison among COE, LPSP, and DL is not distorted by differences in scale, thereby enabling a more objective evaluation of the trade-offs. On the global Pareto front, which consists of non-dominated solutions, a total of 20 points were identified. The Hybrid COA–WCA contributed 4 points, equal to COA and WCA, indicating that the hybrid approach does not merely generate dominated solutions but also contributes to the Pareto envelope and provides competitive compromise

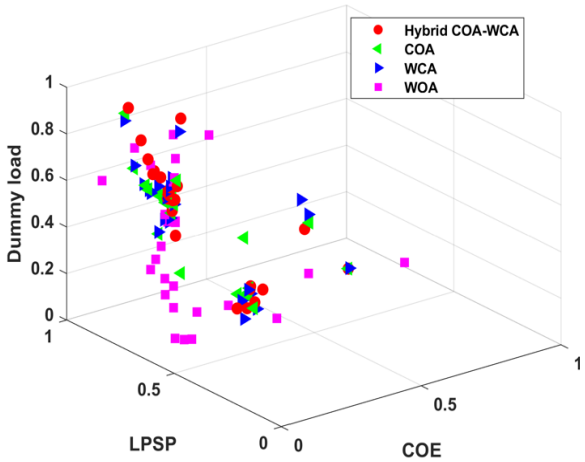

Fig. 9 Pareto fronts obtained by the hybrid COA-WCA and benchmark algorithms, illustrating solution diversity and trade-offs among COE, LPSP, and dummy load.

alternatives. When solution selection is based on weighted scalarization emphasizing reliability (w_COE=0.40, w_LPSP=0.57, w_DL=0.03), the Hybrid approach demonstrates the most stable aggregated performance. It achieves the lowest average aggregated objective function value (mean f=0.4079) and the lowest average scaled LPSP value (0.5896) compared with COA, WCA, and WOA. These results indicate that the Hybrid approach maintains reliability more consistently without significantly compromising cost performance, thereby providing better typical performance across runs, although the absolute best-case solution is still obtained by another algorithm (WOA).

These results indicate that the main advantage of the Hybrid COA–WCA lies not in producing the most extreme solution for a single objective, but in providing a more consistent trade-off among COE, LPSP, and DL. In practical HRES and microgrid planning, this characteristic is particularly important because system design rarely prioritizes cost, reliability, or dummy load independently. Instead, the preferred solution is generally the one that remains competitive across all objectives while maintaining stable performance over repeated runs. In this regard, the hybrid method demonstrates greater relevance for decision-making than algorithms that perform well only in specific objective dimensions.

The superiority of the Hybrid COA–WCA can be attributed to the complementary balance between exploration and exploitation. COA contributes broader global exploration, which helps prevent premature convergence and improves the identification of promising regions in the search space. In contrast, WCA strengthens local exploitation by refining candidate solutions around high-quality regions. Their integration therefore enhances search diversity during the early stage and improves solution refinement during the later stage. This interpretation is consistent with the metaheuristic literature, which shows that hybridization often improves solution quality and reduces performance variability compared with single algorithms. For example, Çetinbaş et al. (2023) reported that the hybrid HHO–AOA improved exploration–exploitation coordination in microgrid optimization, while Janamala et al. (2021) emphasized the strong global search capability of COA. The present findings extend these observations by showing that the combination of COA and WCA can improve the overall compromise quality in a three-objective HRES optimization problem.

A comparison across the individual objectives further clarifies the trade-offs among the algorithms. WOA achieves the lowest mean COE (1.350), indicating its ability to identify highly economical solutions. WCA produces the lowest mean LPSP (226.28), reflecting stronger reliability performance in that objective. In contrast, the Hybrid COA–WCA provides a more balanced performance across LPSP and DL while maintaining competitive cost performance. Although its dummy load is slightly higher, the difference remains relatively small from a practical design perspective when considered together with its stronger robustness and aggregated performance.

From the Pareto front perspective, the Hybrid COA–WCA also exhibits a meaningful distribution of non-dominated solutions. This is important because the quality of a Pareto front depends not only on the number of points, but also on the diversity and practical relevance of the trade-off solutions provided to decision-makers. Previous studies have similarly shown that hybrid methods can improve Pareto front diversity and reduce the risk of local entrapment in multi-objective renewable energy optimization (Bose and Auxillia, 2021; Hossain et al., 2022; Charadi et al., 2023; Belboul et al., 2022).

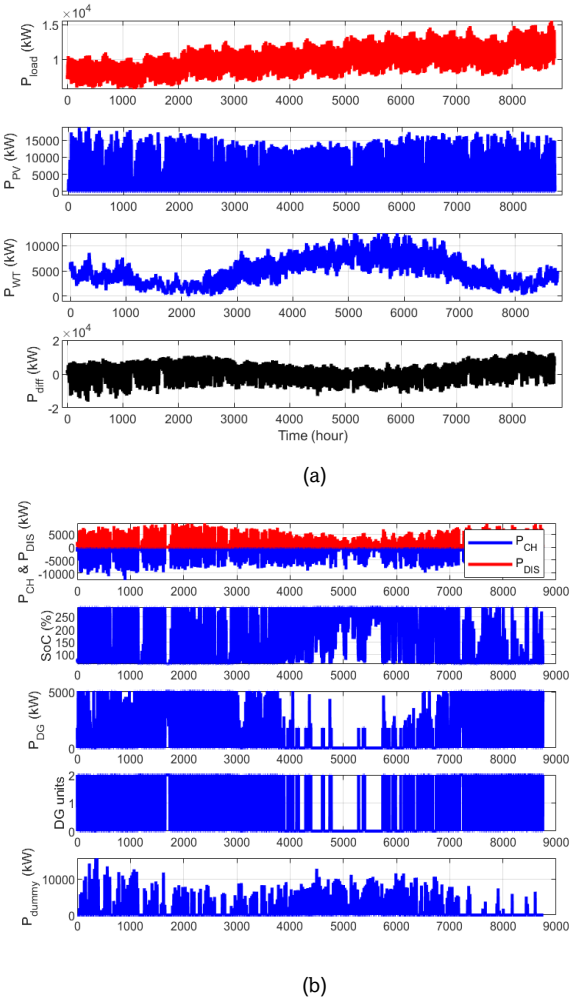

Fig. 10 Load variation and power generation simulation results of the Hybrid COA–WCA algorithm in a hybrid microgrid system over a one-year period (8,760 hours)

Therefore, the present results support the broader view that hybrid metaheuristics are advantageous not only because they improve a single metric, but also because they provide a more informative and stable solution space for stakeholder-based decision-making. Overall, the Pareto front analysis confirms that the Hybrid COA–WCA provides the most balanced and practically relevant performance among the evaluated algorithms.

4.6 Power Supply and Load Balancing

Fig. 10 presents the simulation results of the Hybrid COA-WCA algorithm with respect to the balance between electrical load demand and power generation in a 100% renewable hybrid microgrid system. Under excess generation conditions, the power produced by the solar PV modules and wind turbines exceeds the load demand. Therefore, the surplus energy is used to charge the batteries until the state of charge (SoC) reaches 100%. Any remaining excess power is then diverted to dummy loads.

Conversely, when the power generated by solar and wind sources is insufficient to meet the load demand, the system supplies the deficit using the battery storage, or activates the biodiesel generator when the available battery power is inadequate. In certain operating conditions, a loss of power

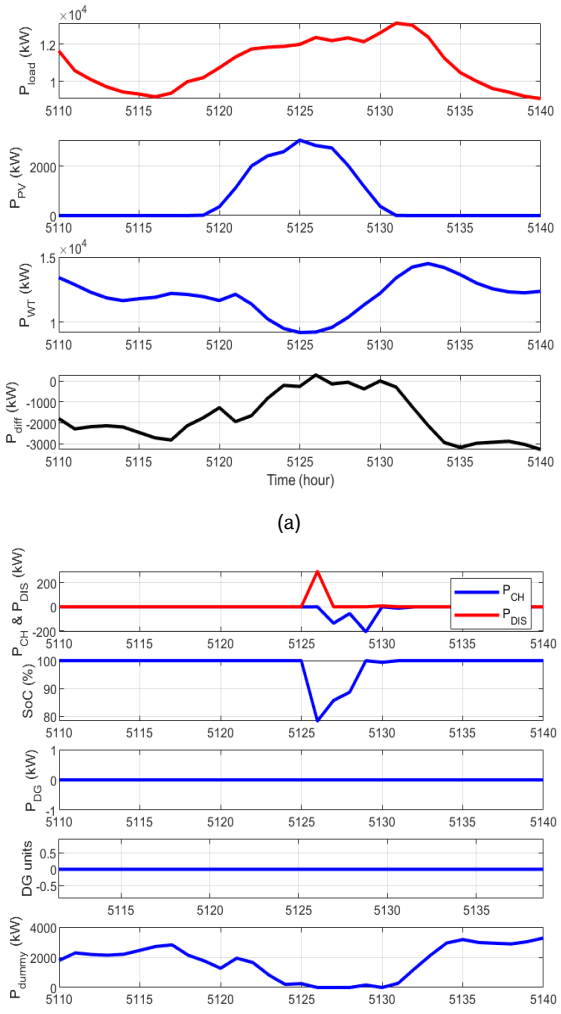

Fig. 11 Hybrid COA–WCA simulation results during the period of highest wind speed variation

supply to the load may occur, which is also considered within the optimization process.

Under conditions where power generation from solar PV modules and wind turbines exceeds the load demand, the biodiesel generator does not operate. The surplus power is first used to charge the battery until the State of Charge (SoC) reaches 100%. Any remaining excess power is then directed to the dummy load. Conversely, when power generation from solar and wind sources is insufficient to meet the load demand, the required power is supplied by the battery system. If the available battery power is also insufficient, the biodiesel generator is activated. In certain operating conditions, a shortage or loss of power supply to the load may occur.

4.6.1 Highest Wind Speed Condition

Fig. 11 presents the simulation results of the Hybrid COA-WCA algorithm over a 30-hour period, from hour 5110 (August 1 at 10:00 PM) to hour 5140 (August 3 at 4:00 AM). During this interval, the highest wind speed variation occurred at hour 5133 (August 2 at 9:00 PM). As shown in Fig. 11 (a), the electrical load decreased from 11,636 kW at hour 5110 to 9,338.32 kW at hour 5115, then gradually increased to 10,739.7 kW and reached a peak value of 13,112.6 kW at hour 5131 (7:00 PM), before decreasing again.

Power generation from the solar PV modules started at hour 5119 and reached a peak value of 3,046.05 kW at hour 5125 (1:00 PM). Thereafter, it gradually decreased to 376.793 kW at hour 2130 and eventually dropped to zero as solar irradiation diminished. Meanwhile, power generation from the wind turbines exhibited a significant increase during this period due to the high wind speed conditions. The wind power output began at 13,426.1 kW at hour 5110 and gradually decreased to its lowest value of 9,192 kW at hour 5125. Subsequently, the power generation increased again and reached a peak of 14,502 kW at hour 5133 (9:00 PM). During this period, the combined power generation from the solar PV modules and wind turbines substantially exceeded the load demand.

A negative power difference ($\boldsymbol{P_{diff}}$) occurs, indicating that the power generated by the solar PV modules and wind turbines exceeds the load demand. Fig. 11 (b) illustrates the variations in battery charging power ($\boldsymbol{P_{CH}}$, kW) and discharging power, the battery State of Charge (SoC, %), the total generated power, the number of operating biodiesel generator units, and the dummy load. Because the power generation from the solar and wind sources exceeds the load demand, the battery SoC remains close to 100% for most of the period. At hour 5126, the SoC decreases to 78.3% when wind turbine generation reaches its minimum, and battery discharging occurs between hours 5125 and 5127. Subsequently, the battery charging process starts at hour 5127 and continues until hour 5130, reaching a maximum charging power of 209 kW.

Under these excess power conditions, power generation from the biodiesel generator is not required. Throughout the 30-hour period, the biodiesel generator does not operate. The surplus power generated results in the activation of the dummy load. When the battery State of Charge (SoC) reaches 100% and excess power is still available, the remaining power is diverted to the dummy load. During this period, a relatively large dummy load is required, starting at hour 5110 (10:00 PM) with a value of 1,789 kW, which then increases to 2,819 kW at hour 5117 (5:00 AM). The dummy load becomes zero between hours 5126 and 5130, and subsequently increases again, reaching its maximum value of 3,273 kW at hour 5140, when wind speed remains high and the load demand is relatively low.

4.6.2 Lowest Wind Speed Condition

Fig. 12 shows the performance of the Hybrid COA–WCA algorithm under the lowest wind speed condition over a 30-hour simulation period. The minimum wind speed of 1.7271 m/s occurred at hour 2125, resulting in a very limited contribution from the wind turbine. During the same period, the load demand fluctuated and reached its maximum value of 10.904 kW at hour 2131, whereas photovoltaic generation was available only during daytime and peaked at hour 2125 before declining to zero. Consequently, the renewable energy supply was unable to consistently match the load profile.

The results indicate that the low-wind condition caused a prolonged supply deficit, as reflected by the positive P_{diff} during most of the interval. Wind turbine output decreased to zero between hours 2124 and 2130, while photovoltaic generation alone was insufficient to compensate for both the loss of wind power and the increasing load demand. Under these conditions, battery charging was highly limited and occurred only briefly around the period of peak solar generation. This indicates that storage operation in this scenario was opportunistic rather than strategic, since the system did not

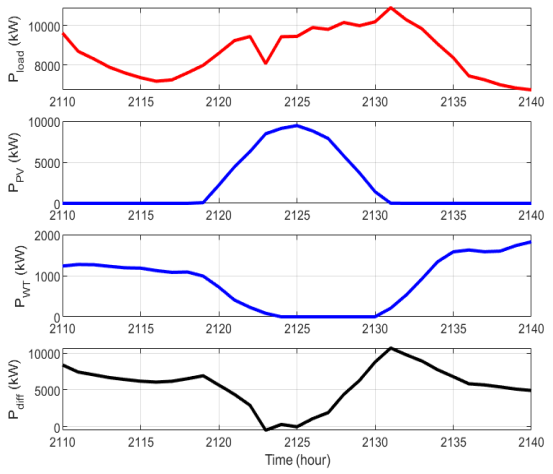

(a)

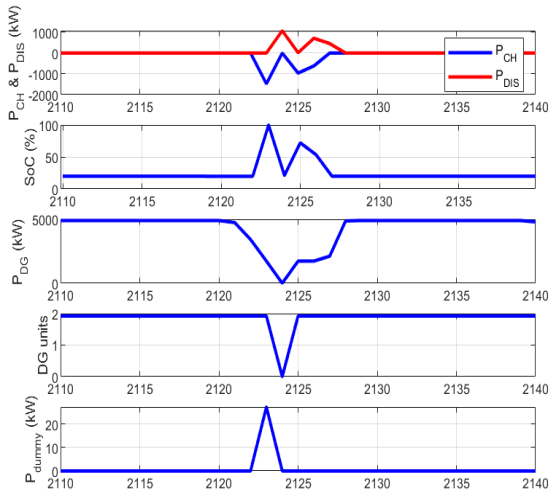

(b)

Fig. 12 Hybrid COA–WCA simulation results during the period of lowest wind speed variation

experience sufficient renewable surplus to support substantial energy accumulation.

The biodiesel generators therefore play a critical role in maintaining supply continuity. However, even with two generator units operating, the total generated power remains insufficient to fully satisfy the load demand, with the maximum deficit reaching 4.868 kW at hour 2130. The absence of dummy load throughout the simulation further confirms that the system operates entirely under deficit conditions, with no excess generation available. These findings indicate that under low-wind-speed conditions, the hybrid system depends strongly on dispatchable backup generation, while the contributions of wind power and battery storage become secondary. More importantly, they show that the proposed optimization strategy prioritizes available renewable resources and minimizes biodiesel usage whenever possible, although overall system performance remains highly sensitive to renewable resource scarcity.

4.7 Implications and Future Research Directions

These findings indicate that algorithm selection should not be based solely on convergence speed, but rather on final solution quality and stability under uncertainty. For microgrid sizing or hybrid energy system design where reliability and realism are critical, Hybrid COA–WCA is a strong candidate because it tends to produce robust, practically plausible configurations (e.g., avoiding excessive battery oversizing) while maintaining consistently superior objective values.

Methodologically, multi-metric evaluation and robustness testing should be treated as standard procedures, since algorithmic performance can shift under non-ideal conditions such as load variability, renewable resource intermittency, and economic parameter uncertainty. A key limitation of this study is that trade-off interpretation remains dependent on the specific formulation of the aggregated objective function and the chosen weights/penalty settings. Future work should therefore investigate: (i) adaptive parameter tuning strategies, (ii) explicit Pareto-based multi-objective optimization to avoid reliance on fixed weighting schemes, and (iii) integration of intelligent decision layers (e.g., fuzzy logic or machine learning) to improve adaptivity to operational dynamics and uncertainty.

6. Conclusion

This study demonstrates the superior performance of the hybrid Coyote Optimization Algorithm and Water Cycle Algorithm (COA-WCA) in optimizing the design and operation of Hybrid Renewable Energy Systems (HRES). The results indicate that COA-WCA outperforms traditional algorithms such as COA, WCA, and the Whale Optimization Algorithm (WOA) in terms of solution quality, convergence speed, and robustness. The main strength of COA-WCA lies in its balanced exploration-exploitation mechanism, which enables it to address the complexities of multi-objective HRES optimization more effectively. Its adaptability to uncertainties in renewable energy generation, together with its ability to minimize key performance metrics such as Cost of Energy (COE), Loss of Power Supply Probability (LPSP), and Dummy Load (DL), provides a more efficient and reliable solution for hybrid microgrid systems. This research contributes to the growing body of knowledge by introducing a hybrid optimization approach that combines the strengths of COA and WCA, offering a more efficient solution for optimizing renewable energy systems. Future studies may extend the applicability of this approach to larger-scale systems, integrate real-time operational frameworks, and enhance computational efficiency for practical deployment. In addition, incorporating stochastic optimization and multi-horizon energy management strategies could further improve the robustness and applicability of the COA-WCA algorithm.

Overall, algorithm selection for microgrid and hybrid energy system design should prioritize solution quality, robustness, and practical feasibility rather than convergence speed alone. The Hybrid COA–WCA method demonstrates strong performance by consistently providing high-quality and feasible solutions. Furthermore, multi-metric evaluation and robustness testing are essential to ensure reliable performance under uncertainty. Future research should address current limitations by exploring adaptive parameter tuning, Pareto-based multi-objective optimization, and intelligent decision-making approaches to improve system adaptability and performance.

References

Akinwola, A.B. and Alkuhayli, A. (2025) Hybrid PSO–Reinforcement Learning-Based Adaptive Virtual Inertia Control for Frequency

Stability in Multi-Microgrid PV Systems, *Electronics (Switzerland)*, 14(17). https://doi.org/10.3390/electronics14173349.

Akter, H., Howlader, H. O. R., Saber, A. Y., Mandal, P., Takahashi, H., & Senjyu, T. (2021) Optimal sizing of hybrid microgrid in a remote island considering advanced direct load control for demand response and low carbon emission, *Energies*, 14(22). https://doi.org/10.3390/en14227599.

Alahakoon, S., Roy, R.B. and Arachchillage, S.J. (2023) Optimizing Load Frequency Control in Standalone Marine Microgrids Using Meta-Heuristic Techniques, *Energies*, 16(13), 4846. https://doi.org/10.3390/en16134846.

Alhawsawi, E.Y., Salhein, K. and Zohdy, M.A. (2024) A Comprehensive Review of Existing and Pending University Campus Microgrids, *Energies* . https://doi.org/10.3390/en17102425.

Aljohani, T.M., Ebrahim, A.F. and Mohammed, O. (2020) Hybrid microgrid energy management and control based on metaheuristic-driven vector-decoupled algorithm considering intermittent renewable sources and electric vehicles charging lot, *Energies*, 13(13). https://doi.org/10.3390/en13133423.

Alsharif, A., Ahmed, A., Khaleel, M.M., Nassar, Y., Sharif, A., and El-Khozondar, H.J. (2023) Whale Optimization Algorithm for Renewable Energy Sources Integration Considering Solar-to-Vehicle Technology, *Proceedings of 2023 IEEE 9th International Women in Engineering (WIE) Conference on Electrical and Computer Engineering, WIECON-ECE 2023*. https://doi.org/10.1109/WIECON-ECE60392.2023.10456379.

Rajagopalan, A., Nagarajan, K., Bajaj, M. (2024. (2024) Multi-Objective Energy Management in a Renewable and EV-integrated Microgrid Using an Iterative Map-Based Self-Adaptive Crystal Structure Algorithm, *Scientific Reports*, 14(1). https://doi.org/10.1038/s41598-024-66644-3.

Azeem, O., Ali, M., Abbas, G., Uzair, M., Qahmash, A., Algarni, A., & Hussain, M. R. (2021) A comprehensive review on integration challenges, optimization techniques and control strategies of hybrid ac/dc microgrid, *Applied Sciences (Switzerland)*, 11(14). https://doi.org/10.3390/app11146242.

Azeem, S. Javed, I. Naseer, O. Ali and Ghazal, T.M. (2025) A New Hybrid PSO-HHO Wrapper Based Optimization for Feature Selection, *IEEE Access*, 13. https://doi.org/10.1109/ACCESS.2025.3570901.

Bakeer, A., Elmorshedy, M.F., Salama, H. (2023) Optimal design and performance analysis of coastal microgrid using different optimization algorithms, *Electrical Engineering*, 105(6). https://doi.org/10.1007/s00202-023-01954-9.

Balasubramanyam, P. and Sood, V.K. (2023) A Novel Hybrid Swarm Intelligence and Cuckoo Search Based Microgrid EMS for Optimal Energy Scheduling, *Distributed Generation and Alternative Energy Journal*, 38(4). https://doi.org/10.13052/dgaej2156-3306.3843.

Bazgan, C., Ruzika, S., Thielen, C. (2022) The Power of the Weighted Sum Scalarization for Approximating Multiobjective Optimization Problems, *Theory of Computing Systems*, 66(1). https://doi.org/10.1007/s00224-021-10066-5.

Belboul, Z., Toual, B., Kouzou, A., Mokrani, L., Bensalem, A., Kennel, R., & Abdelrahem, M. (2022) Multiobjective Optimization of a Hybrid PV/Wind/Battery/Diesel Generator System Integrated in Microgrid: A Case Study in Djelfa, Algeria, *Energies*, 15(10), 3579. Available at: https://doi.org/10.3390/en15103579.

Bhatti, M. Z. A., Siddique, A., Aslam, W., & Atiq, S. (2024) Design and Analysis of a Hybrid Stand-Alone Microgrid, *Energies*, 17(1). https://doi.org/10.3390/en17010200.

Billah, M., Yousif, M. Numan, M., Salam, I.U., Kazmi, S.A.A, and Alghamdi, T.A.H. (2023) Decentralized Smart Energy Management in Hybrid Microgrids: Evaluating Operational Modes, Resources Optimization, and Environmental Impacts, *IEEE Access*, 11. https://doi.org/10.1109/ACCESS.2023.3343466.

Bose, R.B. and Auxillia, D.J. (2021) A robust predictive feedback FPID controller using elephant herd virtual inertia optimization control algorithm in Islanded microgrid, *International Journal of Numerical Modelling: Electronic Networks, Devices and Fields*, 34(5). https://doi.org/10.1002/jnm.2889.

Boukaibat, A., Krami, N., Rochdi, Y., El Bakkali, Y., Laamim, M., & Rochd, A. (2025) Real-Time Energy Management in Microgrids: Integrating T-Cell Optimization, Droop Control, and HIL Validation with OPAL-RT, *Energies*, 18(15). https://doi.org/10.3390/en18154035.

Cetinbas, I., Tamyurek, B. and Demirtas, M. (2022) The Hybrid Harris Hawks Optimizer-Arithmetic Optimization Algorithm: A New Hybrid Algorithm for Sizing Optimization and Design of Microgrids, *IEEE Access*, 10. https://doi.org/10.1109/ACCESS.2022.3151119.

Charadi, S., Chakir, H. E., Redouane, A., El Hasnaoui, A., & El Bhiri, B. (2023) A Novel Hybrid Imperialist Competitive Algorithm–Particle Swarm Optimization Metaheuristic Optimization Algorithm for Cost-Effective Energy Management in Multi-Source Residential Microgrids, *Energies*, 16(19), 6896. https://doi.org/10.3390/en16196896.

Charadi, S., Chakir, H. E., Redouane, A., El Hasnaoui, A., Et-taoussi, M. (2023) Bi-objective optimal active and reactive power flow management in grid-connected AC/DC hybrid microgrids using metaheuristic-PSO, *Clean Energy*, 7(6), 1356–1380. https://doi.org/10.1093/ce/zkad081.

CORE Udayana (2024) *Pemetaan Potensi untuk Nusa Penida 100% Energi Terbarukan*.

Dabhi, D. and Pandya, K. (2020) Metaheuristic Optimization Algorithm for Day-Ahead Energy Resource Management (ERM) in Microgrid Environment of Power System, *Lecture Notes in Electrical Engineering*. https://doi.org/10.1007/978-981-15-0974-2_11.

Pham, M.C., Tran, T.Q., Bacha, S., Hably, A., and An, L.N. (2018) Optimal sizing of battery energy storage system for an islaned microgrid, *Proceedings: IECON 2018 - 44th Annual Conference of the IEEE Industrial Electronics Society*, 1, 1899–1903. https://doi.org/10.1109/IECON.2018.8591391.

Dey, S. and Xu, H. (2023) Intelligent Distributed Swarm Control for Large-Scale Multi-UAV Systems: A Hierarchical Learning Approach, *Electronics (Switzerland)*, 12(1). https://doi.org/10.3390/electronics12010089.

Diab, A.A.Z, Sultan, H.M., Mohamed, I.S., Kuznetsov, O.N., and Do, T.D. (2019) Application of Different Optimization Algorithms for Optimal Sizing of PV/Wind/Diesel/Battery Storage Stand-Alone Hybrid Microgrid, *Ieee Access*, 7, 119223–119245. https://doi.org/10.1109/access.2019.2936656.

Mohamed, M.A.E., Mahmoud, A.M., Saied, E.M.M. (2024) Hybrid Cheetah Particle Swarm Optimization Based Optimal Hierarchical Control of Multiple Microgrids, *Scientific Reports*, 14(1). https://doi.org/10.1038/s41598-024-59287-x.

Eskandar, H., Sadollah, A., Bahreininejad, A., Hamdi, M. (2012) Water cycle algorithm - A novel metaheuristic optimization method for solving constrained engineering optimization problems, *Computers and Structures*, 110–111. https://doi.org/10.1016/j.compstruc.2012.07.010.

Fracas, P., Zondervan, E., Franke, M., Camarda, K., Valtchev, S., & Valtchev, S. (2022) Techno-Economic Optimization Study of Interconnected Heat and Power Multi-Microgrids with a Novel Nature-Inspired Evolutionary Method, *Electronics (Switzerland)*, 11(19). https://doi.org/10.3390/electronics11193147.

Helfrich, S., Herzel, A., Ruzika, S. . (2022) An approximation algorithm for a general class of multi-parametric optimization problems, *Journal of Combinatorial Optimization*, 44(3). https://doi.org/10.1007/s10878-022-00902-w.

Hossain, M.A., Ahmed, T., Hossain, M.S., Dey, P., Ahmed, S., Hossain, M. M. (2022) Optimization of the factors affecting BT-2 black tea fermentation by observing their combined effects on the quality parameters of made tea using Response Surface Methodology (RSM), *Heliyon*, 8(2). https://doi.org/10.1016/j.heliyon.2022.e08948.

Hossam-Eldin, A., Mostafa, H., Kotb, H., AboRas, K. M., Selim, A., & Kamel, S. (2022) Improving the Frequency Response of Hybrid Microgrid Under Renewable Sources' Uncertainties Using a Robust LFC-Based African Vulture Optimization Algorithm, *Processes*, 10(11), 2320. https://doi.org/10.3390/pr10112320.

Hussein, H. M., Rafin, S. M. S. H., Abdelrahman, M. S., & Mohammed, O. A.. (2024) Hardware Implementation of a Resilient Energy Management System for Networked Microgrids, *World Electric Vehicle Journal*, 15(5). https://doi.org/10.3390/wevj15050209.

Ibrahim, I.M., Abdelaziz, A.Y., H. H. Alhelou, H.H., and Omran, W.A. (2023) Sizing of Microgrid System Including Multi-Functional Battery Storage and Considering Uncertainties, *Ieee Access*, 11, 29521–29540. https://doi.org/10.1109/access.2023.3259459.

Jaiswal, S., Sahoo, S.C. and Das, D.C. (2025) Microgrids integrated with diverse energy storage technologies, its challenges and optimized applications: A review, *Suranaree Journal of Science and Technology*, 32(2). https://doi.org/10.55766/sujst7894.

Janamala, V. and Sreenivasulu Reddy, D. (2021) Coyote optimization algorithm for optimal allocation of interline –Photovoltaic battery storage system in islanded electrical distribution network considering EV load penetration, *Journal of Energy Storage*, 41. https://doi.org/10.1016/j.est.2021.102981.

Kharrich, M., Mohammed, O. H., Kamel, S., Selim, A., Sultan, H. M., Akherraz, M., & Jurado, F. (2020) Development and Implementation of a Novel Optimization Algorithm for Reliable and Economic Grid-Independent Hybrid Power System, *Applied Sciences*, 10(18), p. 6604. Available at: https://doi.org/10.3390/app10186604.

Lei, Y., Wang, Z., Wang, D.. (2023) Co-benefits of carbon neutrality in enhancing and stabilizing solar and wind energy, *Nature Climate Change*, 13(7). https://doi.org/10.1038/s41558-023-01692-7.

Marler, R.T. and Arora, J.S. (2010) The weighted sum method for multi-objective optimization: New insights, *Structural and Multidisciplinary Optimization*, 41(6). https://doi.org/10.1007/s00158-009-0460-7.

Mirjalili, S. and Lewis, A. (2016) The Whale Optimization Algorithm, *Advances in Engineering Software*, 95, 51–67. https://doi.org/10.1016/J.ADVENGSOFT.2016.01.008.

Mirtaheri, H., Macaluso, P., Fantino, M., Efstratiadi, M., Tsakanikas, S., Papadopoulos, P., & Mazza, A. (2021) Hybrid forecast and control chain for operation of flexibility assets in micro-grids, *Energies*, 14(21). https://doi.org/10.3390/en14217252.

Mokhtara, C., Negrou, B., Settou, N., Settou, B., Samy, M.M. (2021) Design optimization of off-grid Hybrid Renewable Energy Systems considering the effects of building energy performance and climate change: Case study of Algeria, *Energy*, 219. https://doi.org/10.1016/j.energy.2020.119605.

Mquqwana, M.A. and Krishnamurthy, S. (2024) Particle Swarm Optimization for an Optimal Hybrid Renewable Energy Microgrid System under Uncertainty, *Energies*, 17(2). https://doi.org/10.3390/en17020422.

Naseri, N., El Hani, S., Machmoum, M., Elbouchikhi, E., & Daghouri, A. (2024) Energy Management Strategy for a Net Zero Emission Islanded Photovoltaic Microgrid-Based Green Hydrogen System, *Energies*, 17(9). https://doi.org/10.3390/en17092111.

Nasir, M., Sadollah, A., Choi, Y.H. *al.* (2020) A comprehensive review on water cycle algorithm and its applications, *Neural Computing and Applications*. https://doi.org/10.1007/s00521-020-05112-1.

Pierezan, J. and Dos Santos Coelho, L. (2018) Coyote Optimization Algorithm: A New Metaheuristic for Global Optimization Problems, *2018 IEEE Congress on Evolutionary Computation, CEC 2018 - Proceedings*. https://doi.org/10.1109/CEC.2018.8477769.

Sanajaoba Singh, S. and Fernandez, E. (2018) Modeling, size optimization and sensitivity analysis of a remote hybrid renewable energy system, *Energy*, 143. https://doi.org/10.1016/j.energy.2017.11.053.

Senarathna, T.S.S. and Hemapala, K.T.M.U. (2020) Optimized Adaptive Overcurrent Protection Using Hybridized Nature-Inspired Algorithm and Clustering in Microgrids, *Energies*, 13(13). https://doi.org/10.3390/en13133324.

Sharma, D.K. and Prabhakar, A. (2021) Orthogonal array optimization of the operational parameters for air-cooled cylindrical lithium-ion battery module, *International Symposium on Advances in Computational Heat Transfer*. https://doi.org/10.1615/ichmt.2021.cht-21.180.

Singla, M. K., Gupta, J., Alsharif, M. H., & Jahid, A. (2023) Optimizing Integration of Fuel Cell Technology in Renewable Energy-Based Microgrids for Sustainable and Cost-Effective Energy, *Energies*, 16(11), 4482. https://doi.org/10.3390/en16114482.

Spiegel, M.H. and Strasser, T.I. (2023) A testbed-based approach for the resilience assessment of multi-microgrids, *Elektrotechnik und Informationstechnik*, 140(1). https://doi.org/10.1007/s00502-022-01093-2.

Tarife, R., Nakanishi, Y., Chen, Y., Zhou, Y., Estoperez, N., & Tahud, A. (2022) Optimization of Hybrid Renewable Energy Microgrid for Rural Agricultural Area in Southern Philippines, *Energies*, 15(6). https://doi.org/10.3390/en15062251.

Tjahjana,D.D.D.P., Rachmanto, R.A., Juwana, W.E., Prasojo, Y.J., Prasetyo, S.D, Arifin, Z. (2023) Economic Feasibility of a PV-Wind Hybrid Microgrid System for Off-Grid Electrification in Papua, Indonesia, *International Journal of Design and Nature and Ecodynamics*, 18(4). https://doi.org/10.18280/ijdne.180407.

Tripathi,M., Pathak, N., Chaudhary, V.K., Singh, P., Singh, P.K, Thirumalesh, B.V., Saroj Bala, S., Maurya, A.K, Patel,N, Yadav, B.K.. (2023) Microbial Decolorization of Crystal Violet Dye by a Native Multi-Metal Tolerant Aeromonas caviae MT-1 Isolate from Dye-Contaminated Soil: Optimization and Phytotoxicity Study, *Toxicology International*, 30(1). https://doi.org/10.18311/ti/2023/v30i1/31254.

Twala, S., Ye, X., Xia, X., Zhang, L. (2023) Optimal integration of solar home systems and appliance scheduling for residential homes under severe national load shedding, *Journal of Automation and Intelligence*, 2(4). Available at: https://doi.org/10.1016/j.jai.2023.12.001.

Ullah, K., Jiang, Q., Geng, G., Rahim, S., & Khan, R. A. (2022) Optimal Power Sharing in Microgrids Using the Artificial Bee Colony Algorithm, *Energies*, 15(3), 1067. https://doi.org/10.3390/en15031067.

Ullah, Z., Wang, S., Elkadeem, M., R., and Kotb, K. M. (2023) Optimal Capacity Planning and Analysis of a Sustainable Solar/Wind Microgrid in Rural Areas, *IEEE Green Technologies Conference*. https://doi.org/10.1109/GreenTech56823.2023.10173808.

Upadhyay, S.K. and Bhasker, R. (2025) Cheetah optimization based ANN maximum power point tracking for PV and wind in hybrid AC-DC microgrid, *Engineering Research Express*, 7(2). https://doi.org/10.1088/2631-8695/ade5ee.

Wang, Y., He, X., Liu, Q., Razmjooy, S. (2024) Economic and technical analysis of an HRES (Hybrid Renewable Energy System) comprising wind, PV, and fuel cells using an improved subtraction-average-based optimizer, *Heliyon*, 10(12). https://doi.org/10.1016/j.heliyon.2024.e32712.

Williams, M.J. and Chang, C.K. (2024) The Optimal Integration of Virtual Power Plants for the South African National Grid Based on an Energy Mix as per the Integrated Resource Plan 2019: A Review, *Energies*. https://doi.org/10.3390/en17246489.

Zaheri, S.H., Hosseini, M. and Fathinasab, M. (2024) Well Pattern optimization as a planning process using a novel developed optimization algorithm, *Scientific Reports*, 14(1). https://doi.org/10.1038/s41598-024-78196-7.

Zhong, M., Wang, L., Liu, Z. and Hou, S. (2020) Reliability Evaluation and Improvement of Islanded Microgrid Considering Operation Failures of Power Electronic Equipment,*Journal of Modern Power Systems and Clean Energy*, 8(1). https://doi.org/10.35833/MPCE.2018.000666.

Appendices

Appendix A : *Coyote Optimization Algorithm (COA)*

The Coyote Optimization Algorithm (COA) is a population-based metaheuristic introduced by Pierezan and Coelho (2018) , inspired by the social behavior of coyote packs (*Canis latrans*) (Pierezan and Dos Santos Coelho, 2018). The algorithm models group dynamics, collective learning, and cultural adaptation in changing environments. COA offers several advantages, including a simple algorithmic structure, a balanced exploration–exploitation mechanism, and relatively fast convergence, making it suitable for solving complex nonlinear global optimization problems (Upadhyay and Bhasker, 2025).
The Coyote Optimization Algorithm (COA) is a population-based metaheuristic inspired by the social organization and adaptive behavior of coyotes. In COA, the population is divided into several packs, and each coyote represents a candidate solution in a $\boldsymbol{D}$-dimensional search space. The social condition of the $\boldsymbol{c}$-th coyote in pack $\boldsymbol{p}$at iteration $\boldsymbol{t}$ is expressed as follows:

$$\mathbf{soc}_{\boldsymbol{c}}^{\boldsymbol{p,t}} = [\boldsymbol{x_1}, \boldsymbol{x_2}, \boldsymbol{x_3}, \dots, \boldsymbol{x_D}] \tag{A.1}$$

where $\boldsymbol{D}$ denotes the number of decision variables. The fitness or adaptation of each coyote is evaluated using the objective function:

$$\boldsymbol{fit}_{\boldsymbol{c}}^{\boldsymbol{p,t}} = \boldsymbol{f}\left(\mathbf{soc}_{\boldsymbol{c}}^{\boldsymbol{p,t}}\right) \tag{A.2}$$

A.1 Population initialization

At the beginning of the optimization process, the coyotes are randomly generated within the lower and upper bounds of each decision variable. The initial social condition of the $\boldsymbol{j}$-th variable is defined as:

$$\boldsymbol{soc}_{\boldsymbol{c,j}}^{\boldsymbol{p,t}} = \boldsymbol{lb_j} + \boldsymbol{r_j}\left(\boldsymbol{ub_j} - \boldsymbol{lb_j}\right) \tag{A.3}$$

where $\boldsymbol{lb_j}$ and $\boldsymbol{ub_j}$ are the lower and upper bounds of the $\boldsymbol{j}$-th variable, respectively, and $\boldsymbol{r_j}$ is a uniformly distributed random number in the interval $[\mathbf{0}, \mathbf{1}]$.

3.5.1.2 Alpha coyote and pack social tendency

Within each pack, the coyote with the best fitness is considered the alpha, which represents the dominant local leader. The alpha coyote in pack $\boldsymbol{p}$ at iteration $\boldsymbol{t}$ is determined byP:

$$\boldsymbol{\alpha}^{\boldsymbol{p,t}} = \mathbf{soc}_{\boldsymbol{c}}^{\boldsymbol{p,t}} \quad \text{such that} \quad \boldsymbol{c} = \mathbf{argmin}\boldsymbol{f}\left(\mathbf{soc}_{\boldsymbol{c}}^{\boldsymbol{p,t}}\right) \tag{A.4}$$

for a minimization problem.
In addition, COA models the collective behavior of the pack through its social tendency, which is commonly calculated as the median of the social conditions of all coyotes in the same pack

$$\mathbf{cult}^{\boldsymbol{p,t}} = \mathbf{median}\left(\mathbf{soc}_{\mathbf{1}}^{\boldsymbol{p,t}}, \mathbf{soc}_{\mathbf{2}}^{\boldsymbol{p,t}}, \dots, \mathbf{soc}_{\boldsymbol{N_c}}^{\boldsymbol{p,t}}\right) \tag{A.5}$$

where $\boldsymbol{N_c}$ is the number of coyotes in each pack.

3.5.1.3 Social condition update

The update mechanism in COA is governed by the influence of the alpha coyote and the pack social tendency. Two social difference vectors are first defined as:

$$\boldsymbol{\delta_1} = \boldsymbol{\alpha}^{\boldsymbol{p,t}} - \mathbf{soc}_{\boldsymbol{cr1}}^{\boldsymbol{p,t}} \tag{A.6}$$

$$\boldsymbol{\delta_2} = \mathbf{cult}^{\boldsymbol{p,t}} - \mathbf{soc}_{\boldsymbol{cr2}}^{\boldsymbol{p,t}} \tag{A.7}$$

where $\boldsymbol{cr1}$ and $\boldsymbol{cr2}$ are two coyotes randomly selected from the same pack. Based on these influences, the new social condition of the $\boldsymbol{c}$-th coyote is updated as

$$\mathbf{new\_soc}_{\boldsymbol{c}}^{\boldsymbol{p,t}} = \mathbf{soc}_{\boldsymbol{c}}^{\boldsymbol{p,t}} + \boldsymbol{r_1}\boldsymbol{\delta_1} + \boldsymbol{r_2}\boldsymbol{\delta_2} \tag{A.8}$$

where $\boldsymbol{r_1}$ and $\boldsymbol{r_2}$ are random numbers in $[\mathbf{0}, \mathbf{1}]$. The fitness of the updated social condition is then evaluated by

$$\boldsymbol{new\_fit}_{\boldsymbol{c}}^{\boldsymbol{p,t}} = \boldsymbol{f}\left(\mathbf{new\_soc}_{\boldsymbol{c}}^{\boldsymbol{p,t}}\right) \tag{A.9}$$

If the new solution is better than the previous one, the coyote adopts the updated social condition:

$$\mathbf{soc}_{\boldsymbol{c}}^{\boldsymbol{p,t+1}} = \begin{cases} \mathbf{new\_soc}_{\boldsymbol{c}}^{\boldsymbol{p,t}}, & \text{if } \boldsymbol{new\_fit}_{\boldsymbol{c}}^{\boldsymbol{p,t}} < \boldsymbol{fit}_{\boldsymbol{c}}^{\boldsymbol{p,t}} \\ \mathbf{soc}_{\boldsymbol{c}}^{\boldsymbol{p,t}}, & \text{otherwise} \end{cases} \tag{A.10}$$

3.5.1.4 Birth, death, and transition mechanisms

To maintain diversity and reduce the risk of premature convergence, COA includes biological operators such as birth, death, and pack transition. A new pup is generated from two parent coyotes selected within the same pack, while considering random inheritance and environmental influence. The probabilities of scatter and association are given by:

$$\boldsymbol{P_s = \frac{1}{D}} \quad \text{(A.11)}$$

$$\boldsymbol{P_a = \frac{1-P_s}{2}} \quad \text{(A.12)}$$

These mechanisms allow the offspring to inherit social traits from both parents while preserving stochastic diversity. In addition, coyote migration between packs may occur with a small probability

$$\boldsymbol{P_e = 0.005\, N_c^2} \quad \text{(A.13)}$$

which promotes information exchange among packs and improves global exploration.

Appendix B : Water Cycle Algorithm (WCA)

The Water Cycle Algorithm (WCA), developed by Eskandar et al. (2012), is inspired by natural hydrological processes such as river flow, rainfall, and evaporation. In this algorithm, the best solution is represented as the sea, which acts as an attractor for other candidate solutions represented by rivers and streams. WCA offers strong global exploration capability, relatively fast convergence, and a small number of control parameters, making it widely applicable to renewable energy system optimization and civil engineering problems (Nasir *et al.*, 2020)

.

B.1 Population Initialization

Assume that the optimization problem has $\boldsymbol{N}$ decision variables and a population size of $\boldsymbol{N_{pop}}$. The $\boldsymbol{i}$-th candidate solution can be represented as:

$$\mathbf{X}_{\boldsymbol{i}} = \left[\boldsymbol{x}_{i,1}, \boldsymbol{x}_{i,2}, \dots, \boldsymbol{x}_{i,N}\right], \qquad \boldsymbol{i} = \mathbf{1}, \mathbf{2}, \dots, \boldsymbol{N_{pop}}. \tag{B.1}$$

The quality of each candidate solution is evaluated using the objective (or cost) function:

$$\boldsymbol{C_i} = \boldsymbol{f}(\mathbf{X}_{\boldsymbol{i}}). \tag{B.2}$$

After evaluating all candidate solutions, the best individual is selected as the sea, while the next best individuals are assigned as rivers. The total number of elite individuals consisting of the sea and rivers is denoted by $\boldsymbol{N_{sr}}$. Accordingly, the number of remaining streams is determined by

$$\boldsymbol{N_{stream}} = \boldsymbol{N_{pop}} - \boldsymbol{N_{sr}}. \tag{B.3}$$

To distribute streams among rivers and the sea, the number of streams assigned to the $\boldsymbol{n}$-th river or the sea is made proportional to its flow intensity, which is determined by the corresponding objective function value. This allocation is expressed as follows:

$$\boldsymbol{NS_n} = \mathbf{round}\left(\left|\frac{\boldsymbol{C_n}}{\sum_{k=1}^{N_{sr}} \boldsymbol{C_k}}\right| \boldsymbol{N_{stream}}\right), \tag{B.4}$$

where $\boldsymbol{NS_n}$ is the number of streams flowing toward the $\boldsymbol{n}$-th river or the sea.

B.2 Stream, River, and Sea Updating Mechanism

The main search mechanism in WCA is based on the movement of streams toward rivers and the movement of rivers toward the sea. This mechanism models the natural water flow from higher elevations to lower elevations, which in optimization terms corresponds to the movement of inferior solutions toward better solutions.

When a stream flows directly toward the sea, its position is updated as:

$$\vec{\boldsymbol{X}}^{\boldsymbol{i}}_{\text{stream}}(\boldsymbol{t}+\mathbf{1}) = \vec{\boldsymbol{X}}^{\boldsymbol{i}}_{\text{stream}}(\boldsymbol{t}) + \mathbf{rand} \times \boldsymbol{C} \times \left(\vec{\boldsymbol{X}}^{\boldsymbol{i}}_{\text{river}}(\boldsymbol{t}) - \vec{\boldsymbol{X}}^{\boldsymbol{i}}_{\text{stream}}(\boldsymbol{t})\right) \tag{B.5}$$

where $\boldsymbol{r}$ is a uniformly distributed random number in the interval $[\mathbf{0}, \mathbf{1}]$, and $\boldsymbol{C}$ is a positive constant typically selected in the range $[\mathbf{1}, \mathbf{2}]$.

If a stream is connected to a river, the updating rule becomes:

$$\vec{\boldsymbol{X}}^{\boldsymbol{i}}_{\text{stream}}(\boldsymbol{t}+\mathbf{1}) = \vec{\boldsymbol{X}}^{\boldsymbol{i}}_{\text{stream}}(\boldsymbol{t}) + \mathbf{rand} \times \boldsymbol{C} \times \left(\vec{\boldsymbol{X}}_{\text{sea}}(\boldsymbol{t}) - \vec{\boldsymbol{X}}^{\boldsymbol{i}}_{\text{stream}}(\boldsymbol{t})\right) \tag{B.6}$$

Similarly, the movement of a river toward the sea is formulated as:

$$\vec{\boldsymbol{X}}^{\boldsymbol{i}}_{\text{river}}(\boldsymbol{t}+\mathbf{1}) = \vec{\boldsymbol{X}}^{\boldsymbol{i}}_{\text{river}}(\boldsymbol{t}) + \mathbf{rand} \times \boldsymbol{C} \times \left(\vec{\boldsymbol{X}}_{\text{sea}}(\boldsymbol{t}) - \vec{\boldsymbol{X}}^{\boldsymbol{i}}_{\text{river}}(\boldsymbol{t})\right) \tag{B.7}$$

These three update equations guide the population toward increasingly promising regions of the search space. If a stream obtains a better objective value than the river to which it is connected, their roles are exchanged. In the same manner, if a river or a stream finds a better solution than the sea, that solution replaces the sea. This replacement strategy strengthens exploitation while preserving population adaptability. Fig. 5 illustrates the schematic representation of the movement mechanism of the WCA toward the optimal solution.

B.3 Evaporation Condition and Exploration Enhancement

To prevent the search process from stagnating around a local optimum, WCA employs an evaporation mechanism. Evaporation is triggered when the distance between a river and the sea becomes sufficiently small, indicating that the search agents have converged too closely to the current best solution. The evaporation condition is expressed as follows:

$$\|\mathbf{X}_{\boldsymbol{sea}} - \mathbf{X}_{\boldsymbol{river}}\| < \boldsymbol{d_{max}}, \tag{B.8}$$

or, for a stream flowing near the sea,

$$\|\mathbf{X}_{\boldsymbol{sea}} - \mathbf{X}_{\boldsymbol{stream}}\| < \boldsymbol{d_{max}}, \tag{B.9}$$

where $\boldsymbol{d_{max}}$ is a small threshold controlling the search intensity around the sea. A smaller value of $\boldsymbol{d_{max}}$ encourages a more accurate local search, whereas a larger value increases diversification. In practical implementation, $\boldsymbol{d_{max}}$ is gradually reduced during iterations to tighten the search around the best solution as the algorithm progresses.

3.5.2.2 Rain Process and Generation of New Streams

Once the evaporation condition is satisfied, a rain process is performed to create new streams and reintroduce diversity into the population. A new stream can be randomly generated within the feasible search region according to:

$$\mathbf{X}_{\boldsymbol{stream}}^{\boldsymbol{new}} = \mathbf{LB} + \boldsymbol{rand} \odot (\mathbf{UB} - \mathbf{LB}), \tag{B.10}$$

where **LB** and **UB** are the lower and upper bounds of the decision variables, respectively, and $\odot$ denotes element-wise multiplication. For streams that are regenerated around the sea, a local random search can be performed using:

$$\mathbf{X}_{\boldsymbol{stream}}^{\boldsymbol{new}} = \mathbf{X}_{\boldsymbol{sea}} + \boldsymbol{\sigma}\,\mathbf{randn}, \tag{B.11}$$

where $\boldsymbol{\sigma}$ is the search variance and **randn** is a normally distributed random vector. This operator improves local exploitation around the current best solution while preserving stochastic exploration. In many implementations, a relatively small variance is preferred so that newly generated streams remain near the promising region without excessively restricting the search space.

Appendix C : Whale Optimization Algorithm (WOA)

The Whale Optimization Algorithm (WOA) was introduced by Mirjalili and Lewis (Mirjalili and Lewis, 2016). This metaheuristic algorithm is inspired by the hunting behavior of humpback whales, particularly their bubble-net feeding strategy.. Based on this behavior, WOA models the search process through mathematical operators representing encircling, exploitation, and exploration mechanisms.

C.1 Encircling Prey

Since the exact position of the global optimum is unknown, WOA assumes that the best solution obtained so far represents the prey position. Accordingly, the remaining search agents update their positions relative to the current best agent. This process is expressed as:

$$\vec{D} = \left|\vec{C} \cdot \vec{X}^*(t) - \vec{X}(t)\right| \quad \text{(C.1)}$$

$$\vec{X}(t+1) = \vec{X}^*(t) - \vec{A} \cdot \vec{D} \quad \text{(C.2)}$$

where t denotes the current iteration, $\vec{X}^*$ is the position vector of the best solution found so far, and $\vec{X}$ is the position vector of a whale. The coefficient vectors $\vec{A}$ and $\vec{C}$ are computed as:

$$\vec{A} = 2\vec{a} \cdot \vec{r}_1 - \vec{a} \quad \text{(C.3)}$$

$$\vec{C} = 2\vec{r}_2 \quad \text{(C.4)}$$

where $\vec{a}$ decreases linearly from 2 to 0 over iterations, and $\vec{r}_1$ and $\vec{r}_2$ are random vectors in the range $[0, 1]$.

C.2 Bubble-Net Attacking Mechanism (Exploitation Phase)

To simulate the bubble-net feeding behavior, WOA employs two exploitation strategies:

1) Shrinking encircling mechanism: achieved by reducing the value of $\vec{a}$, thereby narrowing the search region around the best solution.
2) Spiral updating position: whales move along a spiral path toward the prey, expressed as:

$$\vec{X}(t+1) = \vec{D}' \cdot e^{bl} \cdot \cos(2\pi l) + \vec{X}^*(t) \quad \text{(C.5)}$$

where $\vec{D}' = \left|\vec{X}^*(t) - \vec{X}(t)\right|$, b is a constant defining the spiral shape, and l is a random number in $[-1, 1]$.

The selection between these two mechanisms is controlled probabilistically as follows:

$$\vec{X}(t+1) = \begin{cases} \vec{X}^*(t) - \vec{A} \cdot \vec{D}, & p < 0.5 \\ \vec{D}' \cdot e^{bl} \cdot \cos(2\pi l) + \vec{X}^*(t), & p \geq 0.5 \end{cases} \quad \text{(C.6)}$$

where p is a random number in the range $[0, 1]$.

C.3 Search for Prey (Exploration Phase)

WOA also incorporates an exploration mechanism to enhance global search capability. In this phase, whales update their positions relative to a randomly selected agent:

$$\vec{D} = \left|\vec{C} \cdot \vec{X}_{\text{rand}} - \vec{X}(t)\right| \quad \text{(C.7)}$$

$$\vec{X}(t+1) = \vec{X}_{\text{rand}} - \vec{A} \cdot \vec{D} \quad \text{(C.8)}$$

where $\vec{X}_{\text{rand}}$ is the position of a randomly selected whale. This mechanism enables the algorithm to explore diverse regions of the search space and avoid local optima.

For clarity, the pseudocode of the Whale Optimization Algorithm (WOA) is presented below: